Title

Ectopic Expression of α6 and δ GABAA Receptor Subunits in Hilar Somatostatin Neurons Increases Tonic Inhibition and Alters Network Activity in the Dentate Gyrus

Journal

Journal of Neuroscience, 35(49)

ISSN

0270-6474

Authors

Tong, Xiaoping
Peng, Zechun
Zhang, Nianhui
et al.

Publication Date

2015-12-09

DOI

10.1523/jneurosci.2853-15.2015

Peer reviewed

Cellular/Molecular

Ectopic Expression of α6 and δ $GABA_A$ Receptor Subunits in Hilar Somatostatin Neurons Increases Tonic Inhibition and Alters Network Activity in the Dentate Gyrus

Xiaoping Tong,[1,4]* Zechun Peng,[1]* Nianhui Zhang,[1] Yliana Cetina,[1] Christine S. Huang,[1] Martin Wallner,[2,3] Thomas S. Otis,[1,3,5]* and Carolyn R. Houser[1,3]*

Departments of [1]Neurobiology and [2]Molecular and Medical Pharmacology and [3]Brain Research Institute, David Geffen School of Medicine at the University of California, Los Angeles, Los Angeles, California 90095, [4]Department of Anatomy, Histology and Embryology, Shanghai Jiao Tong University School of Medicine, Shanghai 200025, China, and [5]Roche Pharmaceutical Research and Early Development, Neuroscience, Ophthalmology, and Rare Diseases Translational Area, Roche Innovation Center Basel, CH-4070, Basel, Switzerland

The role of $GABA_A$ receptor ($GABA_AR$)-mediated tonic inhibition in interneurons remains unclear and may vary among subgroups. Somatostatin (SOM) interneurons in the hilus of the dentate gyrus show negligible expression of nonsynaptic $GABA_AR$ subunits and very low tonic inhibition. To determine the effects of ectopic expression of tonic $GABA_AR$ subtypes in these neurons, Cre-dependent viral vectors were used to express GFP-tagged $GABA_AR$ subunits (α6 and δ) selectively in hilar SOM neurons in SOM-Cre mice. In single-transfected animals, immunohistochemistry demonstrated strong expression of either the α6 or δ subunit; in cotransfected animals, both subunits were consistently expressed in the same neurons. Electrophysiology revealed a robust increase of tonic current, with progressively larger increases following transfection of δ, α6, and α6/δ subunits, respectively, indicating formation of functional receptors in all conditions and likely coassembly of the subunits in the same receptor following cotransfection. An *in vitro* model of repetitive bursting was used to determine the effects of increased tonic inhibition in hilar SOM interneurons on circuit activity in the dentate gyrus. Upon cotransfection, the frequency of $GABA_AR$-mediated bursting in granule cells was reduced, consistent with a reduction in synchronous firing among hilar SOM interneurons. Moreover, *in vivo* studies of Fos expression demonstrated reduced activation of α6/δ-cotransfected neurons following acute seizure induction by pentylenetetrazole. The findings demonstrate that increasing tonic inhibition in hilar SOM interneurons can alter dentate gyrus circuit activity during strong stimulation and suggest that tonic inhibition of interneurons could play a role in regulating excessive synchrony within the network.

Key words: **dentate hilus; hippocampus; interneurons; nonsynaptic $GABA_A$ receptors; somatostatin-Cre mice**

Significance Statement

In contrast to many hippocampal interneurons, somatostatin (SOM) neurons in the hilus of the dentate gyrus have very low levels of nonsynaptic $GABA_AR$s and exhibit very little tonic inhibition. In an effort to increase tonic inhibition selectively in these interneurons, we used Cre-dependent viral vectors in SOM-Cre mice to achieve interneuron-specific expression of the nonsynaptic $GABA_AR$ subunits (α6 and δ) *in vivo*. We show, for the first time, that such recombinant GFP-tagged $GABA_AR$ subunits are expressed robustly, assemble to form functional receptors, substantially increase tonic inhibition in SOM interneurons, and alter circuit activity within the dentate gyrus.

Introduction

$GABA_A$ receptor ($GABA_AR$)-mediated tonic inhibition is recognized as a major regulator of neuronal activity and could be particularly important for control of neuronal excitability during periods of strong activity (Farrant and Nusser, 2005; Brickley and Mody, 2012; Sun et al., 2013). However, predicting the effects of tonic inhibition on network activity becomes challenging when effects on both principal cells and interneurons are considered

Received July 27, 2015; revised Oct. 23, 2015; accepted Nov. 1, 2015.

Author contributions: X.T., Z.P., M.W., T.S.O., and C.R.H. designed research; X.T., Z.P., N.Z., Y.C., C.S.H., and M.W. performed research; X.T., Z.P., N.Z., M.W., T.S.O., and C.R.H. analyzed data; X.T., Z.P., M.W., T.S.O., and C.R.H. wrote the paper.

This work was supported by National Institutes of Health Grants NS075245 to C.R.H., RR029267 to T.S.O., NS0086076 to T.S.O., and AA021213 to M.W. We acknowledge the Stanford University Gene Vector and Virus Core (supported in part by National Institutes of Health/National Institute of Neurological Disorders and Stroke Grant NS068375) for preparation of the viral vectors. We thank Dr. Mark Kay (Stanford University) for providing the pRC-DJ

(Semyanov et al., 2003; Ferando and Mody, 2014; Lee and Maguire, 2014).

While increasing tonic inhibition in excitatory principal cells is expected to help control their activity and in turn reduce network excitability, the functional effects of tonic inhibition of inhibitory interneurons during strong stimulation are more enigmatic. Viewed from one perspective, tonic inhibition of interneurons, by limiting their activity, could reduce inhibitory control of principal cells and thus contribute to, rather than quell, hyperexcitability within the network (Semyanov et al., 2003; Peng et al., 2004; Lee and Maguire, 2013). An alternate possibility is that enhancing tonic inhibition of interneurons could reduce their rhythmic synchronous firing during periods of strong stimulation and, in doing so, could paradoxically reduce hyperexcitability.

Interestingly, tonic inhibition and the $GABA_A$R subunits that mediate this inhibition differ among principal cells and subgroups of interneurons. Within the dentate gyrus, the δ subunit of the $GABA_A$R is the major mediator of tonic inhibition in granule cells and some interneurons (Glykys et al., 2008; Lee and Maguire, 2013; Yu et al., 2013), including interneurons in the dentate molecular layer and parvalbumin-expressing interneurons along the base of the granule cell layer (Peng et al., 2004; Glykys et al., 2007; Milenkovic et al., 2013). In sharp contrast, the vast majority of somatostatin (SOM) neurons in the dentate hilus lack labeling for either the δ subunit or other $GABA_A$R subunits that are likely to mediate tonic inhibition (Esclapez et al., 1996; Milenkovic et al., 2013). Such observations suggest that these hilar interneurons could have low $GABA_A$R-mediated tonic inhibition.

Hilar SOM neurons, many of which are hilar perforant path-associated cells, are of particular interest because of their key role in controlling granule cell activity through feedback inhibition at dendritic locations, where they are optimally positioned to regulate responses to excitatory input from the entorhinal cortex (Han et al., 1993; Tallent, 2007; Savanthrapadian et al., 2014). If SOM interneurons were to have low tonic inhibition, one might expect these interneurons to be readily activated, thus allowing them to provide reliable inhibitory control of dentate granule cells during normal activity. However, a lack of tonic inhibition could also contribute to their excessive activation during seizure activity. Indeed, hilar SOM neurons are strongly activated during status epilepticus and are particularly vulnerable to seizure-induced damage (Buckmaster and Dudek, 1997; Sun et al., 2007; Houser, 2014).

Considering the importance of hilar SOM neurons and their lack of $GABA_A$R subunits that mediate tonic inhibition, we selectively expressed Cre recombinase (Cre)-inducible GFP-tagged α6 and δ $GABA_A$R subunits using AAV viral transfection *in vivo*. First, we confirmed that $GABA_A$R-mediated tonic inhibition was indeed low in hilar SOM neurons, as suggested by their low levels of $GABA_A$R subunits that are normally associated with tonic inhibition. We then showed that selective ectopic expression of α6 and δ subunits in SOM neurons led to an increase in tonic inhibition selectively in these interneurons, suggesting the formation of functional α6 and δ $GABA_A$Rs. Finally, we show that increasing tonic inhibition in hilar SOM neurons reduces their activation in response to excessive stimulation and alters network activity within the dentate gyrus. Preliminary reports of some of the findings have been presented previously (Peng et al., 2014).

Materials and Methods

Plasmid construction and characterization. Cre-dependent adeno-associated viral (AAV) vectors encoding α6 and δ subunits were constructed so that we could drive expression of the $GABA_A$R in hilar SOM neurons in SOM-Cre mice. These two subunits were selected because receptors containing these subunits are major mediators of tonic inhibition. Although the α4 subunit is commonly associated with the δ subunit in the hippocampus, the α4 and α6 subunits are analogous subunits, and both form strong partnerships with the δ subunit in the forebrain and cerebellum, respectively (Jones et al., 1997; Peng et al., 2002). We chose to express the α6 subunit because it is normally not expressed in the dentate gyrus; thus, any expression that was observed following transfection would most certainly be from the experimentally induced subunit. Also, α6 inclusion gives rise to the highest sensitivity tonic $GABA_A$Rs (Hadley and Amin, 2007; Meera et al., 2011).

C-terminal $GABA_A$R-enhanced green fluorescent protein (eGFP) fusion constructs were made by overlap extension methods with PCR primers (Horton et al., 1989), and PCR products were cloned into a "double-floxed" Cre-inducible AAV vector in antisense orientation with respect to the ubiquitous EF1α promoter. The $GABA_A$R eGFP linker sequences coding for GGRARDPPVAT were inserted in-frame between the last C-terminal amino acid of the $GABA_A$R α6 (human) and the δ (rat) clones and the start codon of eGFP. The Cre-inducible AAV vector (pAAV-EF1a-double floxed-hChR2(H134R)-EYFP-WPRE-HGH pA; plasmid #20298) was obtained from Addgene; the insert (ChR2-eYFP) was removed by cutting with restriction enzymes NheI (5′ end) and AscI (3′ end) and replaced with the NheI AscI cut PCR product coding for the $GABA_A$R subunit α6- and δ-eGFP fusion constructs to obtain Cre-inducible $GABA_A$R-eGFP (α6-eGFP and δ-eGFP) constructs.

For functional testing, inducible $GABA_A$R subunit fusion constructs were cotransfected into HEK293T cells together with a plasmid coding for Cre (pAAV-EF1α-mCherry-IRES-Cre; Addgene, plasmid #55632). Successful Cre-dependent induction was initially demonstrated by fluorescence microscopy with green fluorescence from the Cre-inducible α6-eGFP or δ-eGFP fusion protein and red fluorescence produced by Cre coexpression from an mCherry-IRES-Cre plasmid in HEK293T cells. Numerous double-labeled cells were detected, indicating that each of the $GABA_A$R subunit proteins was expressed in a Cre-dependent manner.

For electrophysiological tests, HEK293T cells were transfected with the Cre-inducible α6-eGFP or δ-eGFP, and with plasmids coding for $GABA_A$R subunits β3 and γ2 for inducible α6-eGFP subunits or α6 and β3 for inducible δ-eGFP, to allow for the formation of functional $GABA_A$R subtypes (α6-eGFP, β3, γ2, or δ-eGFP, α6, β3) in HEK cells. As previously described (Meera et al., 2011), DEAE Dextran HEK cell transfection methods were used to express the human α6, β3, and γ2 subunits driven by the CMV promoter. Receptors with each of the Cre-inducible constructs produced robust GABA-evoked currents in HEK cells (for further details, see Results).

AAV vector production. Each Cre-inducible $GABA_A$R subunit construct was assembled into AAV vectors (AAV-DJ-DIO *Gabra6*-eGFP and AAV-DJ-DIO *Gabrd*-eGFP) by the Stanford University Gene Vector and Virus Core, using AAV-DJ (Grimm et al., 2008). A comparable control virus (AAV-DJ-EF1α-DIO eYFP), containing a construct for eYFP was obtained from the Stanford University Gene Vector and Virus Core.

Animals. All animal-use protocols conformed to the National Institutes of Health guidelines and were approved by the University of California, Los Angeles, Chancellor's Animal Research Committee. Young adult male transgenic mice that express Cre under the control of the SOM promoter (SOM-Cre mice) were used to determine the effects of Cre-dependent viral transfection of α6-eGFP, δ-eGFP, or control eYFP. Animals for breeding were generously provided by Z. Josh Huang and

plasmid used to produce AAV-DJ; Drs. Michael Lochrie and Charu Ramakrishnan (Stanford University) for helpful advice during the initial preparation and testing of the plasmids and AAVs; and Dr. Karl Deisseroth for making reagents available through Addgene.

The authors declare no competing financial interests.

*X.T., Z.P., T.S.O., and C.R.H. contributed equally to this work.

Correspondence should be addressed to Dr. Carolyn R. Houser, Department of Neurobiology, CHS 73-235, David Geffen School of Medicine at University of California, Los Angeles, 10833 Le Conte Avenue, Los Angeles, CA 90095-1763. E-mail: houser@mednet.ucla.edu.

DOI:10.1523/JNEUROSCI.2853-15.2015

 0270-6474/15/3516143-17$15.00/0

Table 1. Antibodies used in this study

Target protein	Species	Source	Catalog #	Concentration	Purpose	References for specificity
α6	Rabbit	Chemicon/Millipore	AB5610	1:1000; 1:25	Light microscopy; Electron microscopy	Glykys et al. (2007), Peng et al. (2013)
δ	Rabbit	Phospho Solutions	868-GDN	1:15	Electron microscopy	Yu et al. (2013)
δ	Rabbit	Millipore	AB9752	1:1000	Light microscopy (double-labeling)	Lee et al. (2014)
Fos	Goat	Santa Cruz Biotechnology	SC-52-G	1:1000	Light microscopy (double-labeling)	Peng and Houser (2005)
GFP	Guinea pig	Frontier Science	GFP-GP-AF1180	1:10000	Light microscopy (double-labeling)	—
Somatostatin	Rabbit	Peninsula	T-4103	1:5000	Light microscopy (double-labeling)	Peng et al. (2013)

Sandra Kuhlman (Cold Spring Harbor Laboratory and University of California, Los Angeles), and these SOM-Cre mice (also referred to as Sst-Cre), on a C57BL/6 background, are now commercially available (stock #013044, The Jackson Laboratory). Some SOM-Cre mice were also bred to Ai9 reporter mice that express the red fluorescent protein (RFP) variant tdTomato following Cre-mediated recombination (stock #007909, The Jackson Laboratory). The generated SOM-Cre × Ai9 mice, 8–12 weeks of age, were used to determine the selectivity and specificity of Cre expression in SOM neurons in the hilus of the dentate gyrus ($n = 4$) and obtain electrophysiological recordings of tonic current from identified SOM neurons ($n = 13$).

Viral vector injections. To selectively label SOM neurons in the dentate hilus, SOM-Cre male mice were injected with a Cre-dependent AAV vector containing either viruses encoding the α6-eGFP and δ-eGFP subunits, singly or in combination, or the control AAV vector containing a construct for eYFP. Mice were anesthetized with isoflurane, and the viral vector was stereotaxically injected in the dentate gyrus with a Nanojet II injector (Drummond Scientific), using glass pipettes. A small animal stereotaxic instrument with digital display console (model 940; Kopf Instruments) was used for positioning of the pipette at the outer part of the hilus, near the border of the granule cell layer. For neuroanatomical and electrophysiological studies, injections were made at three sites in close proximity to each other in the rostral dentate gyrus (−1.6, −1.9, −1.9 mm posterior; 1.0, 1.0, 1.3 mm lateral; 2.25, 2.1, 2.3 mm ventral); and at two sites, each at two depths, in the more caudal dentate gyrus (−3.2, −3.4 mm posterior; 2.8, 2.6 mm lateral; 3.6 and 3.0, 4.2 and 3.4 mm ventral, in relation to bregma) (Paxinos and Franklin, 2001).

For transfection of the $GABA_A$R subunits, injections were made unilaterally in the right hilus of animals used for light microscopic study ($n = 5$ α6-eGFP; $n = 4$ δ-eGFP; $n = 9$ α6/δ-eGFP cotransfection), and electrophysiology ($n = 8$ α6-eGFP; $n = 9$ δ-eGFP; and $n = 12$ α6/δ-eGFP cotransfection), and bilaterally, in the rostral dentate gyrus only, in mice used for electron microscopy ($n = 3$ α6/δ-eGFP). Following the injection, the pipette was left in position for 5 min before it was slowly retracted from the brain. Similar injections were made unilaterally with the control virus (eYFP) for light microscopic ($n = 3$) and electrophysiological studies ($n = 9$). All mice were studied at 4–5 weeks after transfection.

For studies of Fos labeling of transfected cells following pentylenetetrazole (PTZ)-induced seizures, additional mice ($n = 9$) were injected ipsilaterally in the dorsal dentate gyrus with α6/δ-eGFP AAV (cotransfection), and contralaterally, at similar anatomical locations, with the control eYFP AAV. In this set of mice, injections on each side were restricted to the three most rostral sites described above.

Pentylenetetrazole treatment. In α6/δ-eGFP- and control eYFP-transfected SOM-Cre mice (injected bilaterally, as described above), PTZ (45 mg/kg, i.p.) was administered to induce an acute behavioral seizure. The dosage required to elicit behavioral seizure activity was established through prior studies of normal SOM-Cre mice of similar ages ($n = 9$). The behavioral seizures appeared very similar in the control (noninjected) and α6/δ-eGFP-transfected animals. Within 3–7 min following PTZ injections at the selected concentration, the SOM-Cre mice (both control and transfected mice) typically exhibited a single generalized, tonic-clonic seizure that lasted ~30 s. Following the seizure, the animals generally remained quiet, with some head movements but limited locomotion, for the next 50–55 min. At 1 h after the injection, the animals were perfused for immunohistochemical studies of Fos labeling in α6/δ-eGFP-cotransfected and control eYFP-transfected cells.

Tissue preparation for light microscopy. All mice used for neuroanatomical studies were deeply anesthetized with sodium pentobarbital (90 mg/kg, i.p.) and perfused transcardially with 4% PFA in 0.12 M phosphate buffer, pH 7.3. After 1 h at 4°C, brains were removed and postfixed for 1 h. After rinsing, brains were cryoprotected in a 30% sucrose solution overnight at 4°C, embedded in OCT compound (Sakura Finetek), frozen on dry ice, and sectioned at 30 μm with a cryostat (CM 3050S, Leica Microsystems). Brains used for neuroanatomical studies following viral vector injections were sectioned coronally through the rostral (septal) half and then horizontally through the caudal (temporal) half of the hippocampal formation. Transfected brains studied following PTZ-induced seizures were sectioned coronally throughout the hippocampus.

Antibodies. Antibodies used in this study are described in Table 1. The expression and cellular localization of the transfected $GABA_A$R subunits were determined with specific antisera to α6 and δ subunits, using complementary methods of immunoperoxidase labeling for light microscopy, immunofluorescence labeling for confocal microscopy, and immunogold labeling for electron microscopy. Antiserum to SOM was used to determine the correspondence between SOM and RFP-expressing neurons in the hilus, as demonstrated in a SOM-Cre × Ai9 reporter mouse. An antiserum to Fos was used as an indicator of neuronal activation following PTZ-induced seizures in neurons cotransfected for α6/δ-eGFP and in those transfected for control eYFP. For the majority of studies, the transfected neurons were identified by the intrinsic, transfection-induced, eGFP labeling. However, in a subgroup of experiments, this labeling was enhanced with immunofluorescence labeling of eGFP to verify the full extent of transfections.

Immunohistochemistry for light microscopy. Before immunohistochemistry for α6 and δ subunit localization for light microscopy, free-floating sections were processed with a waterbath heating antigen-retrieval method to reduce endogenous peroxidase-like activity and enhance specific labeling of the receptor subunits (Peng et al., 2002). Briefly, the sections were heated to 90°C for 70 min in sodium citrate solution, pH 8.6, and then cooled and rinsed in 0.1 M TBS, pH 7.3. This pretreatment also eliminated the induced eGFP labeling in transfected neurons, thus allowing direct localization of the α6 and δ subunits by immunofluorescence. Following antigen-retrieval methods, sections for light microscopy were processed for immunohistochemical localization of α6 or δ subunits with standard avidin-biotin-peroxidase methods (Vectastain Elite ABC; Vector Laboratories), or immunofluorescence methods, as described in detail previously (Peng et al., 2002, 2004).

Immunofluorescence labeling. Initial studies confirmed that essentially all eGFP-labeled neurons expressed the transfected α6 or δ subunit. Thus, for several double fluorescence labeling studies, the endogenous fluorescence labeling of either tdTomato (a reporter of Cre localization in SOM-Cre × Ai9 mice) or eGFP (an indicator of α6 or δ subunit expression following viral injections in SOM-Cre mice) provided the first fluorescent label. Immunofluorescence methods were then used to label a second marker, either SOM or Fos, in the same sections. These double labeling studies (1) allowed determination of the percentage of SOM neurons that expressed Cre (indicated by RFP) in the hilus of SOM-Cre mice, (2) demonstrated Fos labeling in SOM neurons in nontransfected mice, and (3) demonstrated Fos labeling in α6/δ-eGFP- or control eYFP-transfected neurons. For these studies, sections were incubated for 2 h in 10% NGS to block nonspecific binding sites and 0.3% Triton X-100 to increase reagent penetration. Sections for SOM and tdTomato localization were incubated in SOM antisera (1:5000) for 1 week to maximize penetration of the immunohistochemical reagents, incubated in goat

anti-rabbit IgG conjugated to AlexaFluor-488 (Invitrogen) at room temperature for 4 h, and mounted on slides and coverslipped with antifade medium ProLong Gold (Invitrogen). Similar methods were used for labeling Fos in SOM neurons in nontransfected mice, except that, following incubation in antiserum to Fos and SOM (Table 1), the sections were incubated in a mixture of species-appropriate secondary antisera (donkey-anti goat conjugated to AlexaFluor-555 and donkey anti-rabbit conjugated to AlexaFluor-488, respectively; both from Invitrogen). Similar methods were also used for colocalizing Fos in eGFP or eYFP-labeled cells, except that the incubation in Fos antisera was for 48 h, and the sections were incubated in secondary antiserum, rabbit-anti goat IgG conjugated to AlexaFluor-555 (Invitrogen), for 4 h at room temperature.

While eGFP labeling served as a reliable indicator of α6 and δ subunit transfection in animals with single transfection of each subunit, the eGFP labeling following cotransfection of the two subunits could indicate expression of either or both subunits. Thus, double immunofluorescence labeling for α6 and δ subunits was used to determine whether the two subunits were expressed in the same neurons and had similar cellular localization. For these studies, we developed a new double immunofluorescence labeling method for use of two primary antisera from the same species. This was necessary to use optimal, specific antisera to α6 and δ subunits (both from rabbit). The method used sequential immunofluorescence labeling of each subunit, with the processing for each subunit separated by waterbath heating to eliminate cross-reactivity among the antisera. Sections were first processed with the waterbath antigen retrieval methods described previously to eliminate intrinsic (transfection-induced) eGFP labeling and increase the sensitivity of the primary antiserum binding. After treatment with a blocking solution of 10% NGS, sections were incubated in primary antiserum to the δ subunit (rabbit anti-δ; 1:1000) for 3 nights at room temperature. Following thorough rinsing, sections were incubated in AlexaFluor-555-conjugated goat anti-rabbit IgG for 2 h. Sections were then treated with citrate buffer at 98.5°C for 1 h to eliminate any binding of the subsequent secondary antiserum to the first primary antiserum (rabbit anti-δ). After additional blocking in 10% NGS for 2 h, sections were incubated in the second primary antiserum (rabbit anti-α6; 1:2000) for 3 nights at room temperature and rinsed. Sections were then incubated in AlexaFluor-488-conjugated goat anti-rabbit IgG for 2 h. Numerous control studies confirmed the specificity of the method and demonstrated that the extended waterbath heating eliminated any binding of the second fluorophore-conjugated goat anti-rabbit IgG to the first rabbit antisera. The methodological studies also showed that the intensity of the AlexaFluor-555 was not reduced significantly by the waterbath treatment. (Additional studies of the method demonstrated that the intensity of AlexaFluor-488 was reduced by extended waterbath heating, and thus the AlexaFluor-555-conjugated secondary antisera was used first in this method.)

Tissue preparation for electron microscopy. SOM-Cre mice (4 weeks after AAV-mediated cotransfection of α6/δ-eGFP) were perfused as described for light microscopy, except that a solution of 0.1% glutaraldehyde and 4% PFA was used for tissue fixation. Coronal sections of the forebrain that included the hippocampus were cut at 60 μm on a vibratome (VT1000S; Leica Microsystems).

Immunogold labeling for electron microscopy. Methods for embedding immunogold labeling were similar to those used previously by our laboratory for localization of channelrhodopsin2 (ChR2)-eYFP (Peng et al., 2014). Sections were incubated in primary rabbit antiserum to either α6 (1:25) or δ (1:15) subunits for 48 h, followed by incubation in goat anti-rabbit IgG, conjugated to 1.4 nm colloidal gold particles (1:80; catalog #2004; Nanoprobes), in TBS with 2% NGS for 4 h. After thorough rinsing with TBS and then double-distilled water, sections were processed for 12.5 min in a gold enhancement solution (catalog #2113; Nanoprobes) prepared according to the manufacturer's protocol, as described previously (Wyeth et al., 2012). Immunolabeling controls included omission of either α6 or δ antiserum or colloidal gold-labeled secondary antiserum. No specific immunogold labeling was found in these sections.

Sections were processed for flat embedding as described previously (Zhang and Houser, 1999; Peng et al., 2013). Regions containing the dentate gyrus were trimmed out of the sections and re-embedded on capsules filled with polymerized resin. Ultrathin sections (60–70 nm) were cut with an ultramicrotome (Reichert-Jung) and picked up on nickel mesh grids. Sections were counterstained with a saturated solution of uranyl acetate for 40 min and lead citrate for 4 min. The sections were studied and photographed with a Jeol 100CX II electron microscope at 19,000×.

Analysis of morphological data. Fluorescence-labeled sections were scanned with an LSM 710 (Carl Zeiss) confocal microscope, and confocal images were analyzed with LSM 5 Image Examiner and Zen 2011 imaging software (Carl Zeiss). For detailed analysis of eGFP or α6 or δ subunit expression following AAV injections, confocal *Z*-stack images (~16 slices, 1 μm optical thickness) were acquired (excitation spectra 488 and 555 nm; 20× objective) from the dentate gyrus.

To determine the selectivity and specificity of RFP labeling (used as a reporter of Cre expression) for SOM neurons, the extent of colocalization of these markers was analyzed in the dentate gyrus in SOM-Cre × Ai9 mice ($n = 4$), as described previously in other hippocampal regions (Peng et al., 2014). *Z*-stack images (10–16 slices, 1 μm optical thickness; 20× objective) were acquired in contiguous regions of the dentate gyrus, using the Tile Scan program (Zen 2011, Carl Zeiss). Optical slices were scanned separately for each label, alternating between the two channels (excitation at 488 and 543 nm), in each section throughout the *Z*-stack. Projection images of the dentate gyrus were assembled into a montage, and the hilus, granule cell layer, and molecular layer were delineated. All single- and double-labeled cells were mapped and counted (3 animals × 3 sections per animal × 2 sides = 18 dentate gyrus images). Labeling for both RFP (endogenous) and SOM (immunohistochemical) extended throughout the thickness of the section. Percentages of both RFP and SOM neurons that were double-labeled for the other marker were calculated for the hilus and granule cell/molecular layers of the dentate gyrus. Similar methods were used for evaluating double-labeling of eGFP (endogenous following transfection) and immunolabeling for SOM or the α6 or δ subunits.

The fluorescence intensity of Fos labeling in α6/δ-eGFP and control eYFP-transfected neurons was determined using ImageJ (National Institutes of Health). Digital confocal images (40× objective) were obtained in sections that had not been scanned previously, to eliminate any possible effects of photobleaching. Measurements of fluorescence intensity were made from all subunit-transfected cells and control virus-transfected cells in sections from a region near the site of maximal viral transfection in each of 9 animals. Two-channel *Z*-stacks of images were obtained at 1 μm intervals. The nuclei of eYFP- or eGFP-labeled neurons were outlined with the "freehand selection" tool in a single optical slice in which the nucleus had the largest area. The mean fluorescence intensity of Fos labeling within the nucleus was determined in all α6/δ-eGFP- and control eYFP-transfected neurons within the section. Fluorescence intensity in a small area adjacent to the cell body without any cellular profiles was determined to be background labeling and was subtracted from each measurement. The intensity measurements were analyzed with paired two-tailed Student's *t* test, and $p < 0.05$ was considered significant.

Brain slice preparation. Hippocampal slices were prepared from 10- to 21-week-old SOM-Cre × Ai9 transgenic mice or SOM-Cre mice that had been injected 4–5 weeks earlier with either α6-eGFP or δ-eGFP AAVs or control eYFP AAV. To prepare slices, animals were deeply anesthetized and decapitated, and brains were placed in ice-cold, modified aCSF containing 65 mM sucrose, 82.7 mM NaCl, 2.4 mM KCl, 0.5 mM $CaCl_2$, 6.8 mM $MgCl_2$, 1.4 mM NaH_2PO_4, 23.8 mM $NaHCO_3$, and 23.7 mM D-glucose and saturated with 95% O_2/5% CO_2. This solution also served to cut 300-μm-thick coronal or horizontal slices containing hippocampus and cortex using a VT-1000 vibratome (Leica). Brain slices were allowed to equilibrate for 30 min at 35°C and then switched to 21°C-23°C (room temperature) in normal aCSF containing 126 mM NaCl, 2.5 mM KCl, 1.25 mM NaH_2PO_4, 2 mM $CaCl_2$, 2 mM $MgCl_2$, 26 mM $NaHCO_3$, and 10 mM D-glucose, continuously bubbled with a mixture of 95% O_2/5% CO_2 gas. All electrophysiological studies were executed in the absence of added GABA or NO-711 because ambient GABA in healthy slice preparations could evoke a distinct tonic baseline shift that could be detected when

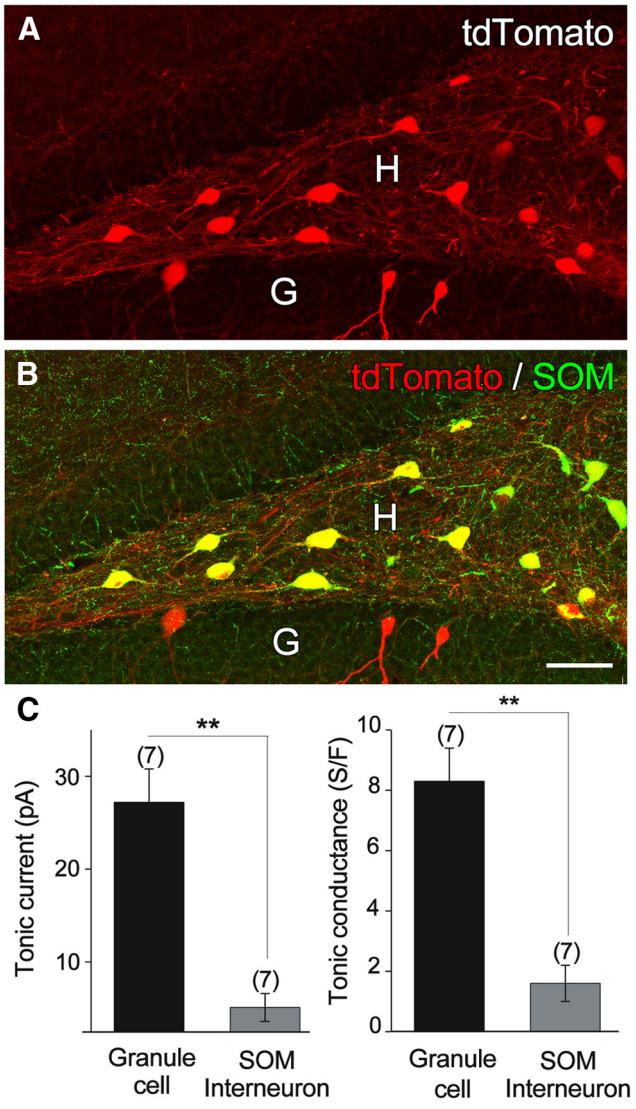

Figure 1. Identified hilar SOM neurons normally exhibit very low tonic inhibition. ***A***, In SOM-Cre × Ai9 mice, tdTomato, a reporter of Cre expression, is present in the cell bodies of numerous neurons in the dentate hilus (H) and a limited number of small neurons in the lower blade of the granule cell layer (G). ***B***, In sections processed for SOM immunohistochemistry, the vast majority of tdTomato-labeled neurons in the hilus are also labeled for SOM, as demonstrated by double labeling (yellow). A few smaller cells within the granule cell layer (G) are labeled only for tdTomato, suggesting extraneous expression in some non-SOM neurons, many of which appear to be granule cells. Electrophysiological recordings were restricted to the hilus where tdTomato labeling reliably identified SOM neurons. ***C***, $GABA_A$R-mediated tonic inhibition was significantly lower in hilar SOM neurons than in dentate granule cells, as indicated by the mean ± SEM comparing tonic current amplitudes and tonic conductances in SOM hilar neurons identified by tdTomato expression compared with unlabeled dentate gyrus granule cells. Tonic current was calculated as SR 95531-sensitive baseline current. Conductance for each cell was calculated based on the current measurements described above divided by the driving force of −70 mV (HP = −70 mV, E_{Cl} = 0 mV); these values were then normalized to cell capacitance for each cell. $^{**}p < 0.01$. Scale bar: ***A***, ***B***, 50 μm.

$GABA_A$Rs were blocked with SR95531. Such conditions were considered the most physiological and avoided the possibility that adding GABA to the bath could desensitize high affinity δ subunit-containing receptors or influence drug modulation of $GABA_A$Rs (Bright and Smart, 2013).

Drug applications. The drugs used in the electrophysiology studies included SR95531, THIP, and DS2 (all from Tocris Bioscience) and kynurenic acid and 4-aminopyridine (4-AP) (both from Sigma-Aldrich). SR95531, THIP, DS2, and 4-AP were dissolved in DMSO and diluted 1:1000 into aCSF before use. For kynurenic acid, we added the powder into the fresh recording buffer at 2 mM working concentration each time.

Electrophysiological recording from brain slices and cultured HEK293 cells. For slice studies of dentate gyrus granule cells and transfected hilar SOM interneurons, cells were recorded in whole-cell mode using pipettes with a typical resistance of 4–5 MΩ when filled with internal solution containing 140 mM CsCl, 4 mM NaCl, 1 mM $MgCl_2$, 2 mM QX-314, 10 mM HEPES, 0.1 mM EGTA, 2 mM Mg-ATP, and 0.3 mM Na-GTP with pH set to 7.3.

For cultured HEK293 cells, GFP-fluorescence-positive HEK293 cells were recorded in whole-cell patch mode with extracellular recording solution comprised of 142 mM NaCl, 8 mM KCl, 6 mM $MgCl_2$, 1 mM $CaCl_2$, 10 mM HEPES, and 10 mM glucose, pH 7.4, and the pipette solution contained 140 mM CsCl, 4 mM NaCl, 0.5 mM $CaCl_2$, 5 mM EGTA, 10 mM HEPES, 2 mM Mg-ATP, and 0.2 mM Na-GTP, pH 7.3 adjusted with CsOH. To elicit maximal activation of $GABA_A$Rs in HEK cells under conditions similar to those experienced by $GABA_A$Rs conducting tonic current, steady-state currents were measured following bath application of GABA (50 μM).

Neurons in all recordings were visualized with an iXon EMCCD camera (Andor Technology) and infrared optics on an upright epifluorescence microscope (Axioskop 2 FS, Zeiss). pCLAMP 8.2 software and an Axopatch-1D amplifier were used for electrophysiology (Molecular Devices). Data were filtered at 2 kHz and acquired at a sampling rate of 20 kHz. Solutions were continuously perfused at a rate of 2 ml/min. All drugs used bath applications for at least 5 min to ensure the effect on the recorded slice.

4-AP model of bursting activity. To generate inhibitory hilar network activity, we relied on the well-characterized 4-AP-induced bursting model. 4-AP (100 μM) was bath applied for 5–8 min before measuring burst parameters. Kynurenic acid (2 mM) was added in the recording buffer to block ionotropic glutamate receptors. To determine the effects of $GABA_A$R modulators on 4-AP induced bursting, THIP (1 μM) or DS2 (10 μM) was added to the bath at 5–10 min after stable bursting patterns were obtained. During preliminary studies, it became apparent that a rundown in burst frequency occurred in slices from both control and α6/δ-transfected animals during the extended period required for evaluating the drug effects on 4-AP-induced bursting. We relied on sham perfusions of an identical duration to the experimental drug perfusions to estimate the baseline rundown in bursting frequency of ~25% at the time the additional drugs were applied (see Fig. 9*D*, dotted line). Thus, all experimental effects of THIP and DS2 were compared with this expected control rundown.

Analysis of electrophysiological data. Tonic $GABA_A$R-mediated current was defined as the steady-state current blocked by saturating concentrations of SR95531, and its magnitude was calculated by plotting all-point histograms of relevant 30 s segments of data. The spontaneous IPSCs (sIPSCs) and 4-AP-induced $GABA_A$R bursts were analyzed by a mini-Analysis 6.0 program. Graphs for all studies were created in OriginPro 8 and assembled in CorelDraw 12. Normally distributed data were analyzed using paired and unpaired Student's two tailed *t* tests and ANOVA, with *post hoc* Tukey–Kramer Multiple Comparison tests, with significance declared at $p < 0.05$. Nonparametric Mann–Whitney rank sum test was used to assess the statistical significance of data deviating from normality. Data are presented as mean ± SEM.

Results

Cre-inducible AAV vectors encoded tagged $GABA_A$R subunits in HEK cells

To test the effectiveness of Cre-inducible $GABA_A$R subunit constructs before packaging in AAV vectors, we used functional and fluorescence measurements in HEK cells that, in addition to GABA subunits, also coexpressed Cre. These experiments rely on the fact that α6 subunit expression is necessary for the formation of functional, pentameric $GABA_A$Rs when expressed with β3 and γ2 in HEK cells. eGFP fluorescence demonstrated protein expression, and electrophysiology confirmed robust GABA-evoked currents upon cotransfection of Cre-inducible $GABA_A$R α6 subunit constructs with those for β3 and γ2. These experiments also confirmed the Cre dependence of the expression vector. Aver-

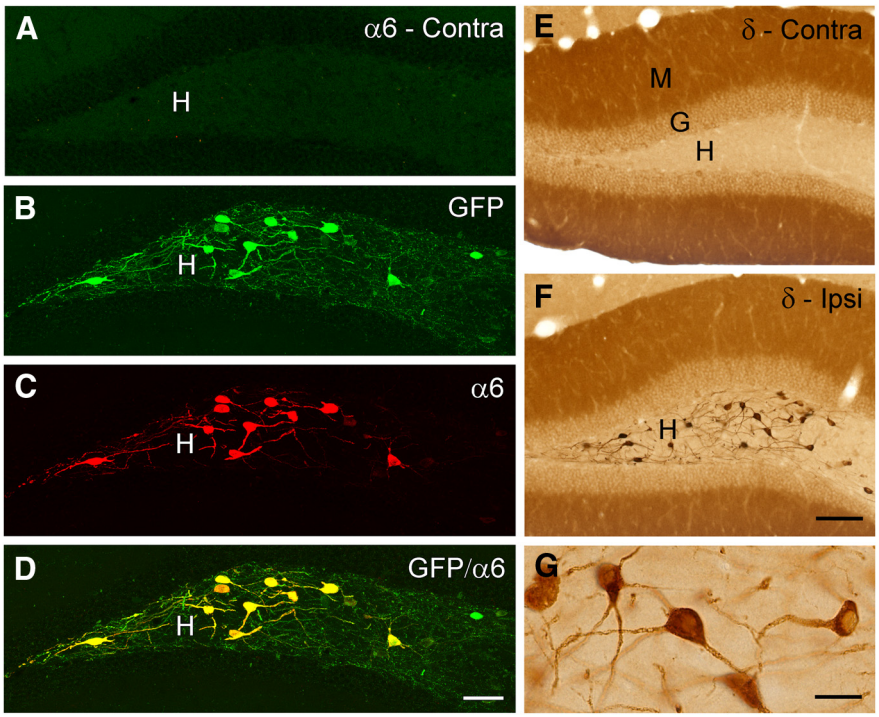

Figure 2. $GABA_A$R α6 and δ subunits were selectively expressed in SOM hilar neurons following single transfection with each Cre-dependent AAV vector. ***A***, The α6 subunit is normally absent in the mouse forebrain, and no immunohistochemical labeling for the α6 subunit is evident in the dentate hilus (H) on the contralateral, nontransfected side. ***B***, In SOM-Cre mice transfected with Cre-dependent α6-GFP AAV, numerous hilar neurons are labeled for GFP, consistent with selective transfection of SOM neurons. ***C***, Immunofluorescence labeling for the α6 subunit demonstrated a similar pattern of neuronal labeling, indicating strong expression of the α6 subunit in the transfected hilar SOM neurons. ***D***, Nearly all GFP-labeled neurons are immunolabeled for the α6 subunit, as shown in the merged image. ***E***, The δ subunit is normally expressed on the dendrites of granule cells in the molecular layer (M) of the dentate gyrus and on interneurons near the base of the granule cell layer (G), as evident on the contralateral side of a transfected animal. Virtually no δ subunit labeling is evident in the dentate hilus. ***F***, In contrast, on the ipsilateral side transfected with δ-GFP AAV, numerous δ subunit-labeled neurons are present in the hilus. ***G***, Immunohistochemical labeling for the δ subunit is present throughout the cytoplasm of the cell bodies and proximal dendrites of transfected neurons. Scale bars: ***A–D***, 50 μm; ***E***, ***F***, 100 μm; ***G***, 25 μm.

age peak currents measured in response to GABA (50 μM) were similar to those obtained with noninducible α6 subunit-containing receptors (Cre-inducible: −374.9 ± 83.3 pA; $n = 13$ cells; standard vector: −354.6 ± 62.4 pA; $n = 5$ cells; $p = 0.86$), confirming the functional expression of the Cre-inducible α6 subunit.

To validate the function of the δ subunit vectors, we could not rely on a similar complementation strategy as δ is not necessary for obtaining functional $GABA_A$Rs; in other words, "binary" α4/6β3 receptors resemble α4/6β3δ subunit-containing receptors in their GABA sensitivity. However, because it has been shown that δ subunit expression is necessary for agonist actions of THIP in δ subunit knock-out mice (Jia et al., 2005), as well as in recombinant α4/6β3δ receptors at concentrations ≤1 μM (Meera et al., 2011), we used THIP at low concentrations (100 nM and 1 μM) to demonstrate functional expression of Cre-inducible δ-eGFP-containing receptors. THIP-induced inward currents were evident in nearly all δ-eGFP/α6β3-Cre transfected cells, but small currents were observed in less than half of negative control cells expressing only α6-eGFP and β3 (δ-eGFP/α6β3-Cre: 10.2 ± 1.7 pA, $n = 16$ of 19 cells at 100 nM THIP; 24.1 ± 6.6 pA, $n = 18$ of 18 cells at 1 μM THIP; control vector: 7.7 ± 1.5 pA, $n = 6$ of 12 cells at 100 nM THIP; 15.5 ± 3.4 pA, $n = 5$ of 12 cells at 1 μM THIP). These findings supported the assembly of functional δ subunit-containing receptors in the HEK cells and thus provided the validation necessary for incorporating the Cre-inducible α6 and δ subunit plasmids in AAV particles for subsequent *in vivo* viral transfections.

Hilar SOM interneurons have low $GABA_A$R-mediated tonic inhibition

Immunohistochemical studies have demonstrated that SOM neurons in the dentate hilus have little or no labeling for several $GABA_A$R subunits that are normally associated with tonic inhibition, including δ, α1, α4, and α6 subunits (Esclapez et al., 1996; Milenkovic et al., 2013; current findings). To determine whether the lack of such subunit labeling is associated with low levels of $GABA_A$R-mediated tonic inhibition, we recorded tonic current in SOM neurons in the hilus of SOM-Cre × Ai9 mice, as identified by tdTomato labeling.

Immunohistochemical studies of these reporter mice confirmed that 97.6% of the tdTomato-labeled neurons in the hilus were labeled for SOM, whereas 98.9% of SOM neurons were labeled for tdTomato ($n = 297$ cells in 18 dentate images from 3 mice; Fig. 1*A*,*B*). Thus, SOM neurons within the hilus could be identified reliably by endogenous tdTomato labeling for electrophysiological recording *in vitro*. A similar high correspondence between tdTomato and SOM labeling was not observed in the granule cell and molecular layers where small numbers of tdTomato-labeled neurons with morphological features of granule cells were not colabeled for SOM (Fig. 1*A*,*B*). Electrophysiological recordings were thus restricted to tdTomato-labeled neurons that were clearly within the hilar region.

Whole-cell recordings demonstrated low tonic current in the labeled hilar neurons (5.1 ± 1.5 pA, $n = 7$ cells; Fig. 1*C*). In comparison, mean tonic current recorded from dentate granule cells was significantly larger (27.2 ± 3.6 pA, $n = 7$ cells; $p = 0.0001$; Fig. 1*C*). When recordings were normalized for cell size (indicated by capacitance) and converted to conductances, tonic conductance densities were significantly larger in dentate granule cells than in SOM interneurons (8.3 ± 1.1 S/F and 1.6 ± 0.6 S/F, respectively, $n = 7$ cells per group; $p = 0.0002$; Fig. 1*C*). These findings are consistent with a lack of immunohistochemical labeling of $GABA_A$R subunits that mediate tonic inhibition in these interneurons. Similar results have been reported previously in abstract form (Wei et al., 2013).

The very low levels of tonic inhibition in this group of SOM neurons provided an *in vivo* target for studying the localization and functional effects of AAV-delivered α6 and δ $GABA_A$R subunits in a subgroup of GABAergic interneurons.

α6 and δ subunits were expressed ectopically in hilar SOM neurons following Cre-dependent transfection in SOM-Cre mice

In the first set of studies, either the α6-eGFP or δ-eGFP subunit was introduced singly in the dentate hilus, using stereotaxic injection of Cre-dependent AAV vectors into the hilus of SOM-Cre

mice. Subunit expression was monitored by eGFP fluorescence and by immunohistochemical labeling of each subunit.

Figure 2*A* shows that no specific labeling of the α6 subunit was observed in the contralateral, nontransfected hilus of SOM-Cre mice, consistent with a normal lack of α6 subunit expression in the forebrain (Fritschy and Mohler, 1995). However, numerous hilar interneurons were strongly labeled for eGFP in SOM-Cre mice following AAV-mediated transfection of the α6 subunit (Fig. 2*B*). Expression of the α6 subunit was verified by immunohistochemical labeling of the subunit (Fig. 2*C*). A very high correspondence was found between eGFP and α6 subunit labeling (Fig. 2*D*). Virtually all GFP-labeled cells were colabeled for α6, and the intensity of labeling for eGFP and the subunit protein varied in parallel.

Delta subunit labeling is normally present throughout the dentate molecular layer where it is localized on granule cell dendrites, but virtually no δ subunit labeling is evident on hilar neurons (Peng et al., 2004). A similar pattern was evident on the nontransfected side of the SOM-Cre mice (Fig. 2*E*). Following Cre-dependent transfection of the δ-eGFP subunit, numerous labeled neurons were evident throughout the hilus (Fig. 2*F*). In the δ subunit-transfected mice, hilar interneuron labeling appeared quite strong compared with the moderately dense labeling that is normally present in the dentate molecular layer (Fig. 2*F*), and labeling was present throughout the cytoplasm of the cell bodies and extended into numerous dendritic processes (Fig. 2*F*,*G*). Little or no immunolabeling was evident in axons and terminal fields.

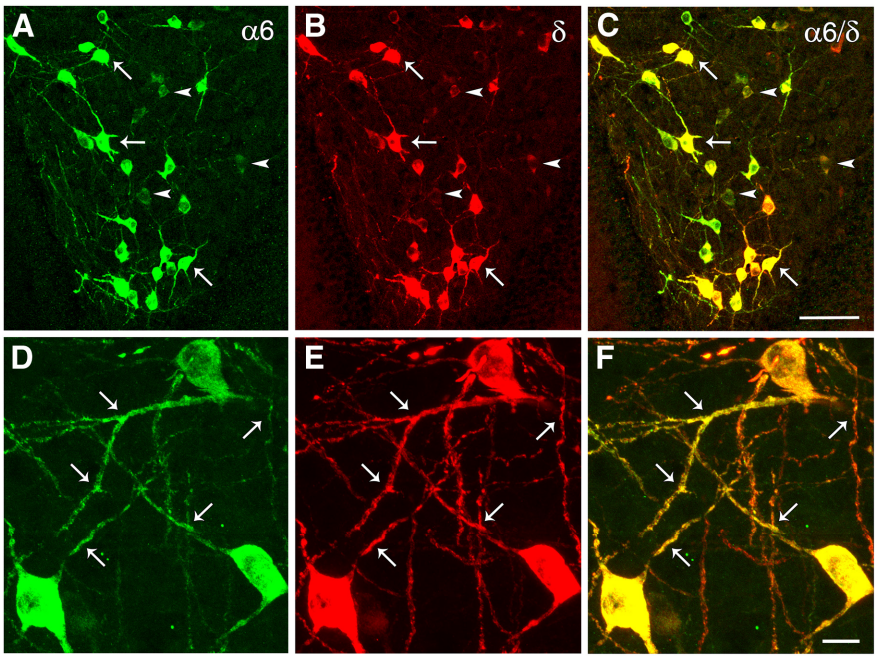

Figure 3. $GABA_A$R α6 and δ subunits have similar localization patterns following cotransfection for the two subunits. ***A–C***, Following immunofluorescence labeling for the α6 and δ subunits in cotransfected animals, a high percentage of hilar neurons are double-labeled for the two subunits. Neurons that are strongly labeled for one subunit are generally strongly labeled for the other subunit (examples at arrows). Neurons with low levels of expression for either subunit often show low or trace labeling for the other subunit but could appear to be single-labeled at lower magnifications (examples at arrowheads). ***D–F***, The patterns of α6 and δ subunit labeling are remarkably similar, not only in neuronal cell bodies but also along dendritic processes (examples at arrows), as emphasized by the merged images in ***F***. Scale bars: ***A–C***, 50 μm; ***D–F***, 10 μm.

Successful expression of the α6 and δ subunits individually led us to determine whether both subunits could be expressed following cotransfection with the two viral vectors. Based on α6/δ subunit partnership in cerebellar granule cells (Jechlinger et al., 1998), we anticipated that the two subunits could assemble in the same $GABA_A$R following injection of both AAV vectors in the hilus. However, it remained possible that the Cre-dependent expression of one subunit might exclude expression of the other or the attached eGFP portions might interfere with assembly of both α6-eGFP and δ-eGFP in the same functional $GABA_A$R. In such instances, the subunits could be expressed in different neurons or in different locations in the same cell. Therefore, we studied the labeling patterns for both subunits with double immunofluorescence confocal microscopy.

Following cotransfection, both α6 and δ subunits were selectively expressed in hilar neurons, and labeling for the two subunits strongly overlapped (Fig. 3*A–F*). The vast majority of neurons that were labeled for one subunit were also labeled for the other subunit. In 11 sections from 7 cotransfected mice, a total of 166 hilar neurons were labeled. The majority of these neurons were double-labeled for the two subunits (155 of 166; 93.9%), while 8 neurons (4.82%) appeared to be single-labeled for the δ subunit and 2 (1.2%) were single-labeled for the α6 subunit. Importantly, the labeling patterns, including the labeling of dendritic processes, appeared very similar for the two subunits (Fig. 3*D–F*). The intensity of labeling for the subunits was not compared because of numerous variables, including different sensitivities of the primary subunit antibodies, different secondary antisera, and different virus titers.

Tissue from cotransfected animals was then studied with electron microscopy to verify that both α6 and δ subunits were localized along the plasma membrane and to determine whether labeling was present at synaptic or nonsynaptic locations. Pre-embedding immunogold labeling was used to determine the localization of the α6 and δ subunits separately, but in the same cotransfected animal. Labeling for each subunit was also evident along the plasma membrane (Fig. 4*A*,*D*). For both α6 and δ subunits, immunogold particles were localized predominantly at extrasynaptic (Fig. 4*A–D*, arrows) or perisynaptic locations (Fig. 4*B*,*C*,*E*,*F*, arrowheads). Immunolabeling was seldom observed directly at synaptic contacts (Fig. 4*B*,*C*,*E*,*F*, open arrowheads). As suggested by light microscopy, immunogold labeling for each subunit was abundant within the cytoplasm, likely reflecting $GABA_A$R proteins in their biosynthetic pathway.

As pre-embedding immunogold methods allowed only single labeling, it was not possible to determine whether the two subunits were localized at precisely the same subcellular sites. However, the similar patterns of labeling, including similar distributions within the neurons and the predominantly nonsynaptic localization of both subunits, are consistent with incorporation of the two subunits within the same $GABA_A$Rs.

Ectopically expressed α6 and δ subunits induced $GABA_A$R-mediated tonic inhibition in SOM-Cre neurons

Electrophysiological studies were then conducted to determine the effects of transfecting each subunit separately and in combination on tonic inhibition. To control for any effects of viral

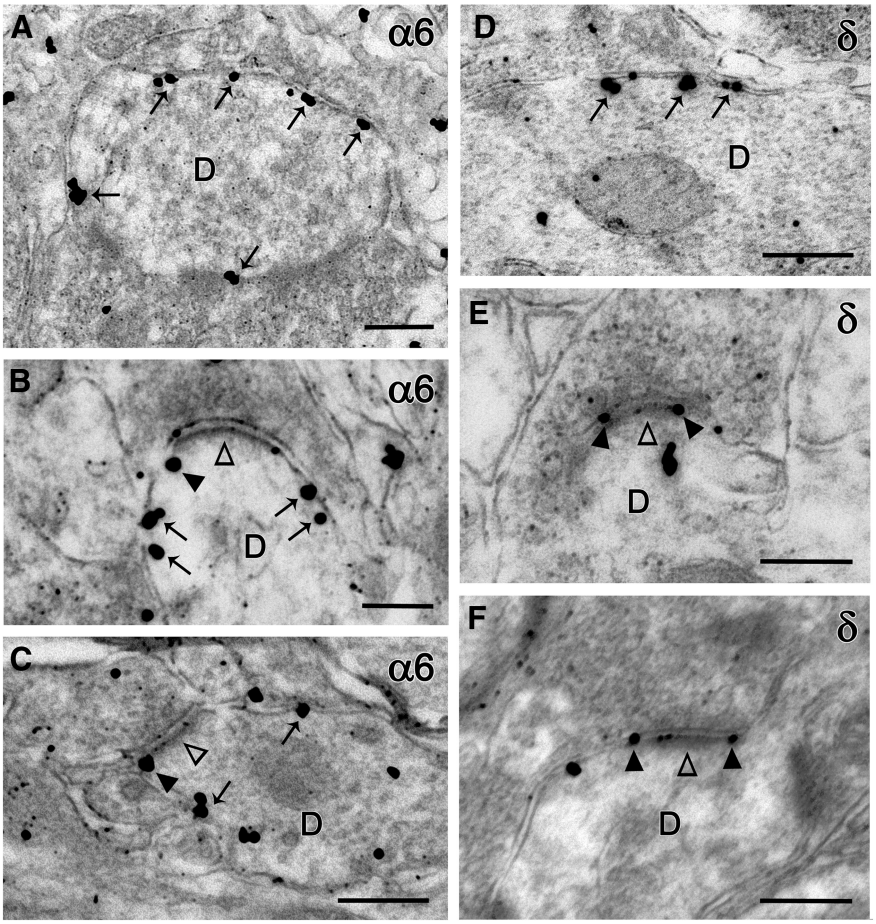

Figure 4. Electron microscopy demonstrates immunogold labeling of α6 (***A–C***) and δ (***D–F***) subunits on the surface of hilar SOM neurons in cotransfected animals at 4 weeks after transfection. ***A***, α6 immunogold labeling is present along the plasma membrane of a dendritic profile (D) within the hilus. ***B***, ***C***, α6 labeling is evident at extrasynaptic locations (example at arrows), and some immunogold particles are located at perisynaptic sites (arrowheads), near a symmetric synapse (open arrowhead). ***D***, Immunogold labeling of the δ subunit is present along the membrane surface (examples at arrows). ***E***, ***F***, δ subunit labeling is evident primarily at nonsynaptic locations, including perisynaptic sites (arrowheads) near symmetric synapses (open arrowheads). Scale bars: ***A***, ***B***, ***E***, ***F***, 0.25 μm; ***C***, ***D***, 0.20 μm.

transfection alone, tonic current was determined in SOM-Cre hilar neurons transfected with Cre-dependent AAV delivering only eYFP. Mean tonic current in such control neurons was low, ranging from 1.2 to 8.5 pA (3.7 ± 0.5 pA; $n = 18$ cells; Fig. 5*A*,*B*). These findings confirmed our previous findings of low levels of tonic inhibition in identified hilar SOM interneurons in SOM-Cre × Ai9 mice (Fig. 1*C*).

Tonic inhibition was then analyzed in $GABA_A$R subunit-transfected neurons, identified by eGFP fusion to the indicated subunit. In each group of subunit-transfected neurons (δ, α6, or α6/δ-cotransfected), the tonic current was significantly larger than that in control neurons transfected with eYFP alone (δ vs YFP, $p < 0.05$; α6 vs YFP, $p < 0.001$; α6/δ vs YFP, $p < 0.001$; ANOVA, with *post hoc* Tukey–Kramer Multiple Comparison tests; Fig. 5*A*,*B*; Table 2), and tonic conductances showed similar differences (Fig. 5*A*,*B*; Table 2). Furthermore, the size of the mean tonic currents and conductances differed among the subunit-transfected groups (Fig. 5*A*,*B*). Compared with that in control-transfected neurons, tonic conductance was 7.6-fold larger in δ subunit-transfected neurons; 14.3-fold larger in α6-transfected neurons; and 28.4-fold larger in α6/δ-transfected neurons (Table 2). Neurons transfected for the α6 subunit showed a trend toward larger tonic current and tonic conductance than those transfected for the δ subunit, but the differences were not statistically significant ($p > 0.05$; ANOVA). Neurons cotransfected for α6 and δ subunits showed significantly larger tonic currents and conductances than those transfected for only the δ ($p < 0.001$) or α6 subunit ($p = 0.01$; ANOVA; Table 2). As expected given the increased tonic GABA conductance, input resistance was decreased in the cotransfected neurons. Input resistance was 374.0 ± 41.1 MΩ ($n = 18$ cells) in YFP control and 210.8 ± 31.5 MΩ ($n = 13$ cells) in α6/δ-cotransfected hilar neurons, a significant difference (unpaired two-tailed *t* test, $p = 0.0063$). Based on the findings above, subsequent electrophysiological experiments focused primarily on the functional responses of SOM hilar neurons in animals cotransfected with α6 and δ subunits.

The significantly larger tonic current in cotransfected neurons suggested that the two subunits had formed partnerships in the same $GABA_A$Rs. To verify the functional expression of the δ subunit in the cotransfected neurons, we studied responses to the $GABA_A$R agonist THIP (1 μM), which at low concentrations is a selective agonist at δ subunit-containing $GABA_A$Rs (Jia et al., 2005; Meera et al., 2011). In control (eYFP-transfected) hilar neurons, SR95531-sensitive tonic current (control) as well as baseline tonic plus THIP-induced additional current (for method of measurement, see Fig. 6) were quite low (4.3 ± 0.8 pA, and 8.6 ± 0.9 pA, respectively, $n = 11$ cells; Fig. 6*A*), consistent with undetectable δ subunit expression in these neurons. Significantly larger currents in control and in THIP were confirmed in δ subunit-transfected neurons (21.0 ± 3.1 pA and 41.0 ± 5.1 pA, respectively, $n = 7$ cells, $p = 0.0012$ and $p < 0.0001$ compared with eYFP-transfected control neurons). In α6/δ-cotransfected neurons, control and 1 μM THIP consistently yielded large currents (Fig. 6*B*; 75.5 ± 19.8 pA and 138.8 ± 30.9 pA, respectively, $n = 6$ cells, $p = 0.0002$ and $p < 0.0001$ compared with eYFP-transfected control neurons). This THIP-induced current was not only considerably larger than that in control neurons but also threefold larger than that in δ subunit-transfected neurons. The large current induced by low doses of THIP in cotransfected neurons provided further support for partnership of the α6 and δ subunits in functional $GABA_A$Rs in these neurons.

Increased tonic inhibition was accompanied by alterations in phasic inhibition in α6/δ subunit-transfected neurons

The presence of substantially larger tonic current in α6/δ-transfected cells, and the fact that SOM hilar neurons contact one another, led us to consider possible alterations in phasic inhibition, which we set out to address through analyses of sIPSCs. These sIPSCs were discernible on baseline current with associated "noise" that appeared to differ between control and α6/δ-transfected neurons (Fig. 7*A*). Such noise was quantified by calculating the variance in the baseline current amplitude from

periods between sIPSCs, showing that in cotransfected hilar neurons baseline noise was increased relative to that in eYFP-transfected neurons (variance, $SD^2 \pm SEM = 16.6 \pm 1.5\ pA^2$, control, $n = 14$ cells; $104.7 \pm 25.6\ pA^2$, α6/δ, $n = 10$ cells; $p = 0.0005$, unpaired t test). The $GABA_A$R antagonist SR95531 abolished this effect (variance $= 12.8 \pm 1.5\ pA^2$, control, $n = 14$ cells; $18.1 \pm 4.5\ pA^2$, α6/δ, $n = 10$ cells; $p = 0.2215$, unpaired t test). These findings are consistent with a large, maintained increase in tonic inhibition in the cotransfected neurons, as described above.

Consistent with no increase in the number or efficacy of postsynaptic $GABA_A$Rs, IPSC amplitude was not altered in the α6/δ-cotransfected neurons compared with eYFP-transfected controls (32.9 ± 2.6 pA, control, $n = 14$ cells; 33.9 ± 2.7 pA, α6/δ, $n = 10$ cells; $p = 0.7446$; Fig. 7*B*). However, consistent with a reduction of presynaptic hilar SOM neuron activity and the fact that these interneurons innervated one another, sIPSC frequency was significantly lower in the α6/δ-cotransfected neurons (1.6 ± 0.3 Hz, control, $n = 14$; 0.4 ± 0.1 Hz, α6/δ, $n = 10$; $p = 0.0043$, unpaired t test; Fig. 7*C*). Despite the apparent decrease in sIPSC frequency, it is possible that some of the smaller phasic currents may have been difficult to detect due to the increase in noise in the transfected neurons.

The mean IPSC decay time was significantly prolonged in α6/δ-cotransfected neurons compared with control (YFP-transfected) SOM hilar neurons (Fig. 7*D*). Most sIPSCs fit to a single exponential decay. However, we reanalyzed the kinetics data by using weighted decay (Wei et al., 2003). The weighted decay times in YFP control and α6/δ-transfected SOM hilar neurons were as follows: 14.5 ± 1.3 ms ($n = 14$ cells); 22.7 ± 3.5 ms ($n = 10$ cells), respectively (unpaired two-tailed t test, $p = 0.021$; Fig. 7*D*). The prolongation of the sIPSC decay suggests that transfected subunits, probably α6, are able to participate in phasic synaptic signaling, consistent with observations indicating that α6 subunits contribute to synaptic currents in cerebellar granule cells (Santhakumar et al., 2006). Our electron microscopy demonstrated immunolabeling of both subunits at perisynaptic sites; thus, the longer decay times also could reflect spillover of GABA at perisynaptic sites (Wei et al., 2003). However, we cannot exclude limited localization of the α6 subunit at synapses. The clear changes at the level of single SOM interneurons led us to explore whether the introduction of nonsynaptic $GABA_A$R subunits might alter the activity of interconnected networks of hilar interneurons under different circumstances.

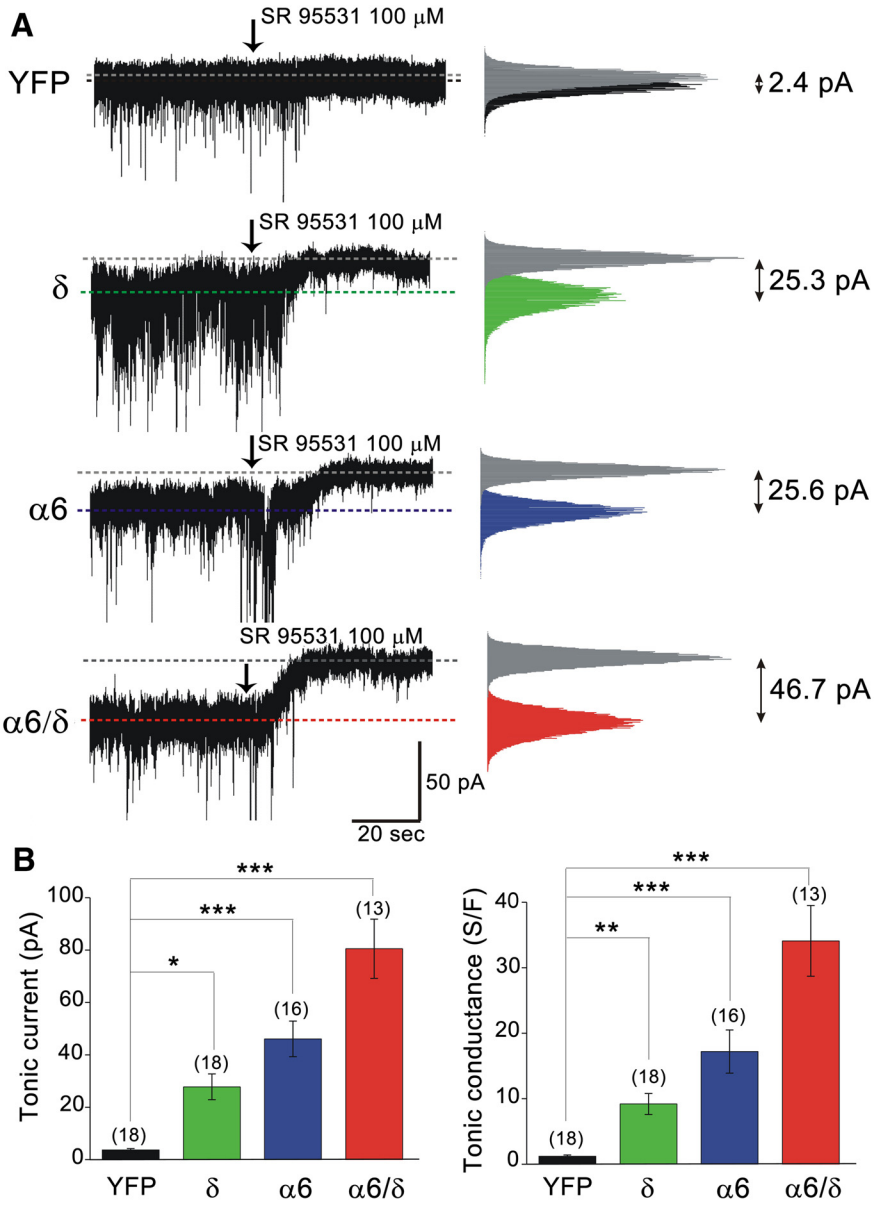

Figure 5. Tonic inhibition is substantially increased in hilar SOM neurons upon Cre-dependent viral expression with tagged δ and α6 subunits. ***A***, Representative traces showing SR 95531-sensitive currents in hilar SOM neurons, which were transfected with YFP as a control, δ, α6, or α6/δ subunits, respectively. Tonic $GABA_A$R-mediated current is defined as the steady-state current blocked by 100 μM SR95531. To the right, all-point histograms of relevant 30 s segments of data are displayed from each cell. ***B***, Bar graphs summarize the average tonic currents and tonic conductances for the indicated transfection conditions. Significantly larger tonic currents are observed relative to control transfections (YFP) upon expression of the δ, α6, and α6/δ subunits. $^*p < 0.05$. $^{**}p < 0.01$. $^{***}p < 0.001$.

Enhancing tonic inhibition in hilar SOM neurons altered circuit activity in the dentate gyrus

Our major question was whether an increase in tonic inhibition of SOM neurons could lead to altered activity of their target granule cells during strong stimulation of the hilar SOM neurons. A well-established model of synchronous hilar network neuron activity is produced by bath application of the potassium channel blocker 4-AP, causing repetitive bursting activity of interneurons within the dentate gyrus that can be observed as giant synchronous IPSCs recorded in granule cells (Avoli et al., 1996; Grosser et al., 2014). Furthermore, these SR 95531-sensitive giant IPSCs are known to be maintained when ionotropic glutamate receptors are blocked, indicating that the activity can be driven solely by

Table 2. Tonic currents and conductances in labeled neurons from control and $GABA_A$R subunit-transfected SOM-Cre mice[a]

Transfections	Tonic current (pA)	Tonic conductance (S/F)	No. of cells	*p* (ANOVA) (tonic conductance) δ	α6	α6/δ	Fold difference (tonic conductance) compared with YFP control
YFP (control)	3.7 ± 0.5	1.2 ± 0.2	18	<0.01	<0.001	<0.001	
δ subunit-GFP	27.8 ± 4.9	9.2 ± 1.6	18		>0.05	<0.001	7.6
α6 subunit-GFP	46.1 ± 6.8	17.2 ± 3.3	16			<0.01	14.3
α6/δ subunits-GFP	80.5 ± 11.3	34.1 ± 5.4	13				28.4

[a]Data are mean ± SEM.

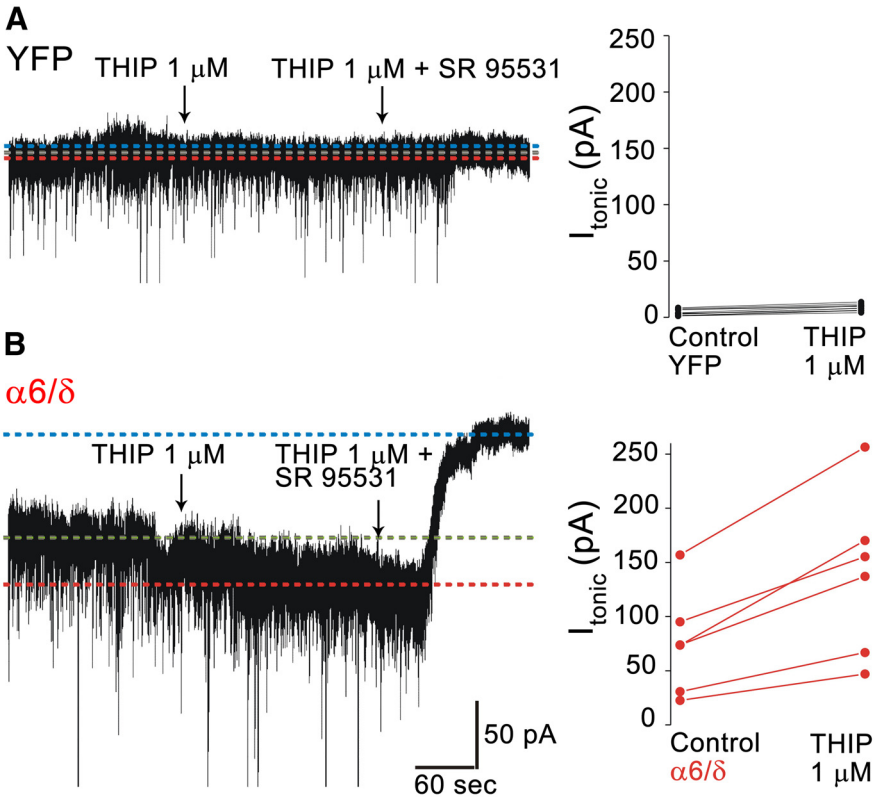

Figure 6. Low concentrations of the δ subunit-selective $GABA_A$R agonist THIP activated GABA current in α6/δ-cotransfected, but not in YFP-transfected, hilar SOM neurons. ***A***, Traces represent minimal current activation by 1 μM THIP and negligible SR 95531-sensitive tonic current in SOM neurons transfected with YFP control. To the right, summary data indicate no SR 95531-sensitive tonic currents ("Control YFP") nor THIP-activated currents in a population of 11 neuron recordings. ***B***, In contrast, transfection of SOM hilar neurons with α6/δ subunits leads to substantial SR 95531-sensitive tonic currents ("Control α6/δ") and THIP-evoked currents. Blue dashed line indicates baseline current. Green dashed line indicates the pre-THIP control level of tonic current. Red dashed line indicates the increased level of current activated by THIP. To the right are results from individual SOM interneurons for which control tonic GABA currents are calculated by subtracting blue from green, and 1 μM THIP current levels are calculated by subtracting blue from red; subtracted values are then expressed as positive current amplitudes.

synchronized activity of interconnected GABAergic interneurons (Grosser et al., 2014). We hypothesized that increased tonic inhibition of the SOM interneurons resulting from α6/δ delivery could reduce their excitability and thus their synchronous firing, leading, in turn, to a decrease in $GABA_A$R-mediated bursts in dentate granule cells. To test this, we pharmacologically isolated IPSC bursts by recording from granule cells in the continuous presence of 4-AP (100 μM) and kynurenic acid (2 mM) to block ionotropic glutamate receptors. Regular, repetitive bursting activity was recorded in dentate gyrus granule cells from both control- and α6/δ-transfected SOM-Cre animals (Fig. 8*A*). While there was no significant difference in the amplitude of the bursts (1419 ± 130 pA, control, $n = 23$ cells; 1258 ± 123 pA, α6/δ, $n = 19$ cells; $p = 0.3816$; Fig. 8*B*), the frequency of the 4-AP-induced bursts was significantly decreased in the α6/δ subunit-transfected slices compared with eYFP-transfected control slices (3.5 ± 0.1 bursts/min, wild-type, $n = 23$ cells; 2.7 ± 0.2 bursts/min, α6/δ, $n = 19$ cells; $p = 0.0001$; Fig. 8*A*,*C*).

We then tested the effects of two pharmacological agents that influence $GABA_A$R-mediated tonic inhibition. In the first set of studies, submicromolar THIP was bath applied during 4-AP-induced bursting. In a second set of studies, DS2, a δ subunit-selective-positive allosteric modulator (Wafford et al., 2009; Jensen et al., 2013), was similarly applied. During studies of 4-AP bursting frequency, a slight time-dependent rundown of ~25% occurred over time periods of 10–15 min (see Materials and Methods); thus, all data were compared with "sham perfusion" data obtained at identical time points indicating no drug effect (Fig. 9*D*, dotted line). For both THIP and DS2, no effects on the mean amplitude of the bursts were observed when comparing predrug versus postdrug conditions in slices from either wild-type or α6/δ-transfected mice. However, a significant decrease in burst frequency was evident in granule cells of slices from α6/δ-transfected animals that were treated with DS2 but not in those treated with THIP (Fig. 9*C*,*D*). Neither drug had significant effects on burst frequency of granule cells in wild-type slices (Fig. 9*B*,*D*).

We chose THIP and DS2 as reagents that show the clearest selectivity for δ-containing $GABA_A$Rs. THIP competitively binds to the GABA agonist site, whereas DS2 is an allosteric modulator and thus is capable of generating a much higher level of tonic current. With this in mind, our working hypothesis is that the GABA concentration during 4-AP-driven activity is high enough that a competitive agonist is much less effective than an allosteric modular. The lack of complete suppression of granule cell bursting by DS2 could be related to the transfection of only a portion of the hilar SOM neurons, varying levels of subunit expression among the transfected neurons, and potential contributions of other $GABA_A$R subunits to the bursting process.

These findings demonstrate that increasing $GABA_A$R-mediated tonic inhibition in hilar SOM interneurons, through ectopic expression of the α6 and δ subunits in these neurons, can alter circuit activity within the dentate gyrus. Moreover, application of the δ subunit-selective-positive allosteric modulator DS2 further reduced the bursting frequency in slices from $GABA_A$R subunit-transfected animals but not in controls, consistent with a contribution of δ subunit-containing $GABA_A$Rs to the reduction of bursting.

Fos labeling was reduced in α6/δ subunit-expressing hilar SOM neurons following induced seizure activity

To determine whether ectopic expression of α6/δ subunits could alter the response of hilar SOM neurons *in vivo*, PTZ was administered systemically to induce a brief seizure episode. During such induced seizures, neurons are strongly activated in many brain regions, including the dentate gyrus, but the seizures are not severe enough to produce neuronal damage.

Fos labeling was used to identify neurons that were strongly activated, as described previously in response to PTZ administration (Li et al., 2014) and spontaneous seizures (Peng and Houser, 2005). In preliminary studies, Fos labeling was evaluated in SOM-Cre mice with no transfections ($n = 4$). At 1 h after brief (~30 s) generalized behavioral seizures, strong Fos labeling was evident in a high percentage (76%) of SOM neurons in the dentate hilus (Fig. 10). The percentages of SOM cells that were strongly labeled for Fos were similar on the two sides (77% and 74%). In addition, numerous granule cells were labeled for Fos in a subgroup of animals. Importantly, the overall patterns of Fos labeling in the dentate gyrus were bilaterally symmetrical in the nontransfected animals.

To determine whether cotransfection of the α6/δ subunits would alter the pattern of Fos labeling, hilar SOM neurons were transfected for Cre-dependent AAV encoding α6/δ subunits (tagged with eGFP) on one side and transfected with Cre-dependent AAV encoding eYFP on the contralateral side. Fos labeling was evaluated qualitatively and by measurements of fluorescence intensity in each labeled neuron, and the mean intensity of labeling in neurons on the two sides was compared.

On the control side of the 9 transfected animals, numerous eYFP-labeled neurons (Fig. 11*A*,*E*) were labeled for Fos, and many of these control-transfected neurons exhibited strong Fos labeling (Fig. 11*C*,*G*). Thus, the labeling of neurons on the control-transfected side closely resembled that in nontransfected SOM-Cre mice.

In contrast, the α6/δ-eGFP-transfected neurons (Fig. 11*B*,*F*) showed less extensive Fos labeling (Fig. 11*D*,*H*). In some animals, Fos labeling of α6/δ-cotransfected neurons was light or absent (Fig. 11*D*), whereas Fos labeling of control-transfected

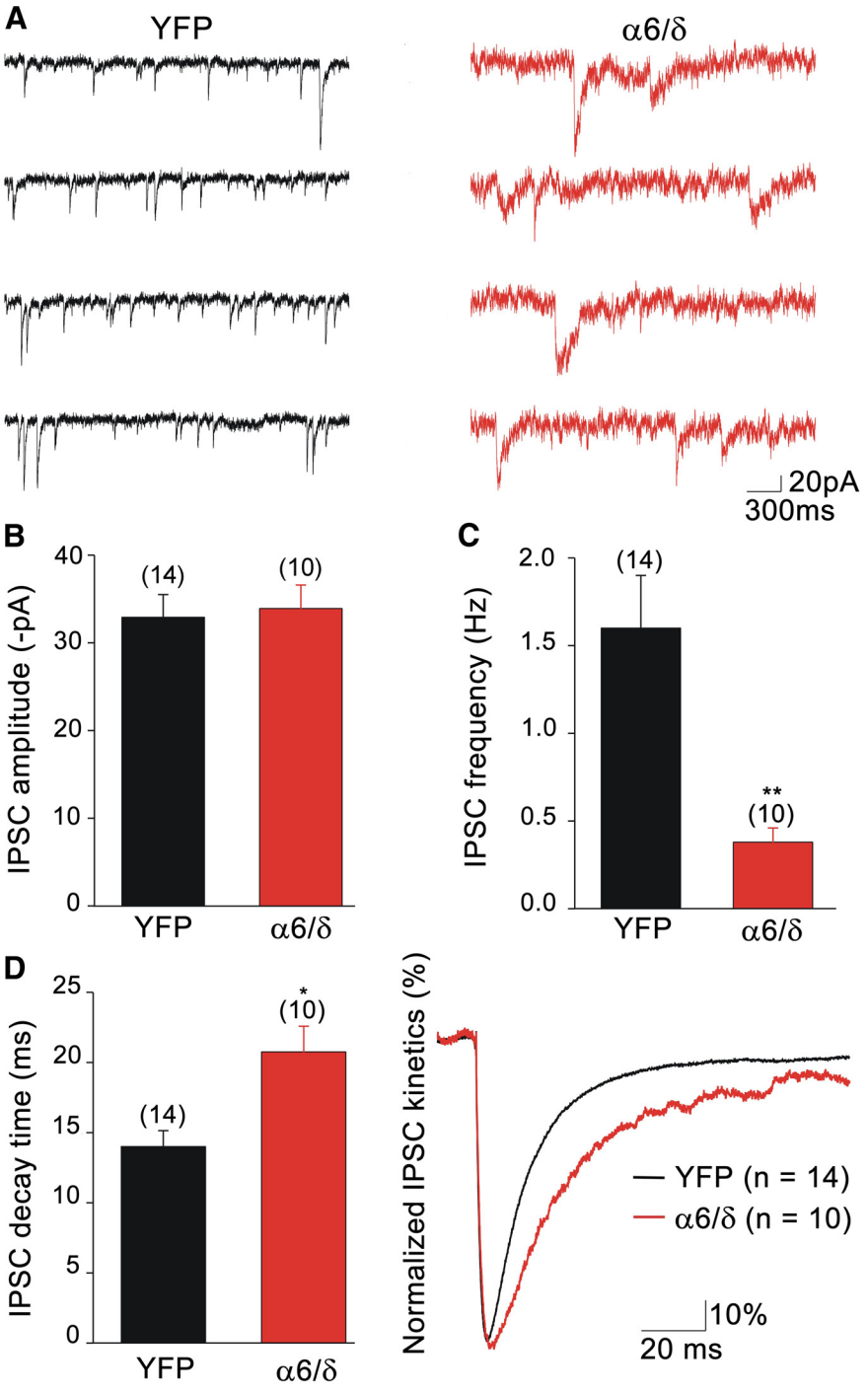

Figure 7. Phasic inhibition is altered following cotransfection of α6 and δ subunits in SOM hilar neurons. ***A***, Representative traces showing sIPSCs in SOM hilar neurons transfected with YFP (black) or with α6/δ subunits (red). In addition to slower and less frequent sIPSCs, baseline "noise" is increased in α6/δ-cotransfected neurons. ***B***, ***C***, Group data comparing YFP-transfected and α6/δ-cotransfected SOM hilar neurons indicate no differences in mean sIPSC amplitudes (***B***) but significantly reduced mean sIPSC frequency (***C***) upon α6/δ expression. ***D***, Mean sIPSC decay time is significantly prolonged in α6/δ-cotransfected compared with control (YFP-transfected) SOM hilar neurons, indicating that ectopically delivered α6/δ subunits may participate in phasic synaptic signaling. $*p < 0.05$. $**p < 0.01$.

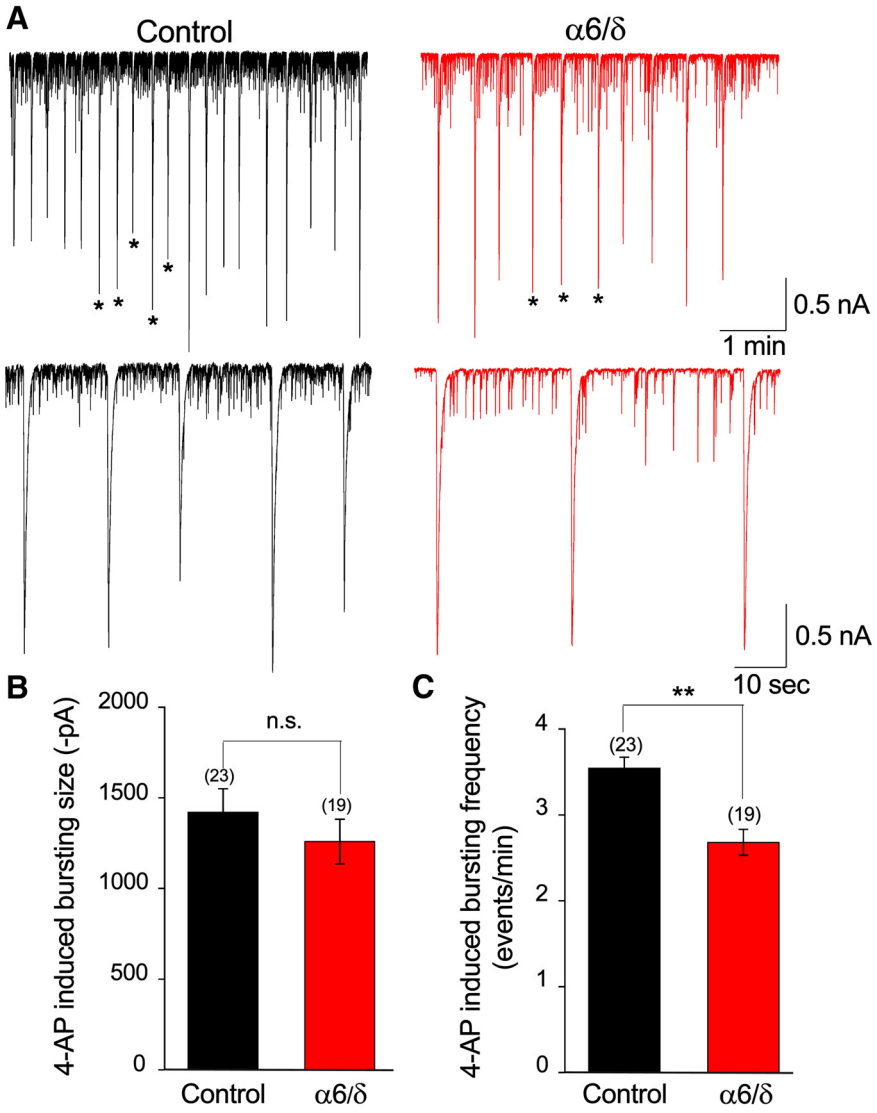

Figure 8. Enhancing tonic inhibition in hilar SOM neurons alters network activity impinging on dentate gyrus granule cells. ***A***, Top, Representative traces recorded from dentate granule cells of giant IPSC bursts induced by 4-AP (100 μM). Hilar SOM interneurons were either transfected with YFP (control, black) or transfected for $\alpha6/\delta$ subunits (red). Top, Slower time base. Asterisks indicate the events shown below at faster timescale. Bottom, Faster time base. ***B***, ***C***, Mean amplitudes and frequencies of 4-AP-induced bursting indicate that $\alpha6/\delta$ cotransfection has no effect on burst amplitude but slows bursting frequency. $^{**}p < 0.01$. n.s., Not significant.

neurons in the same section was strong (Fig. 11*C*). In other animals, often with Fos labeling in granule cells (suggesting greater activation of the dentate gyrus), Fos labeling in the transfected interneurons was light to moderate (Fig. 11*H*) but appeared lower than Fos labeling of control neurons on the contralateral side of the same section (compare Fig. 11*G*,*H*). Measurements of the fluorescence intensity of Fos labeling confirmed these observations. The mean (±SEM) fluorescence intensity of Fos labeling was significantly higher in eYFP-transfected neurons than in $\alpha6/\delta$-eGFP-cotransfected neurons (34.9 ± 5.8 vs 8.8 ± 3.0 intensity units, respectively; $n = 9$ animals; 88 eYFP-labeled neurons and 66 $\alpha6/\delta$-eGFP-cotransfected neurons; $p = 0.0001$, two-tailed paired t test). Thus, the mean fluorescence intensity of Fos labeling was 76.6% lower in the $\alpha6/\delta$-transfected neurons than in eYFP-labeled control neurons on the contralateral side. These findings suggest that transfection of the $\alpha6/\delta$ $GABA_A$R subunits and an associated increase in tonic inhibition limit the strong activation of SOM interneurons that normally occurs during acute, induced seizure activity *in vivo*.

Discussion

The major findings of this study are as follows: (1) $GABA_A$R-mediated tonic inhibition is quite low in SOM interneurons in the hilus of the dentate gyrus, consistent with virtual absence of the δ subunit and other $GABA_A$R subunits that normally mediate tonic inhibition; (2) ectopic expression of the $\alpha6$ and δ subunits of the $GABA_A$R specifically in hilar SOM interneurons leads to the formation of functional receptors that induce substantial tonic inhibition in these interneurons; and (3) the increased tonic inhibition in hilar SOM interneurons alters circuit activity in the dentate gyrus during strong stimulation both *in vitro* and *in vivo*.

$GABA_A$R-mediated tonic inhibition is extremely low in hilar SOM neurons

The present findings demonstrate conclusively that SOM neurons in the dentate hilus normally have low $GABA_A$R-mediated tonic inhibition. Interestingly, SOM interneurons in the somatosensory cortex also show low tonic inhibition, a similar lack of δ subunit expression, and lack of modulation by low concentrations of THIP (Vardya et al., 2008). The functional significance of very low levels of tonic inhibition in some classes of interneurons is unknown, but one suggestion is that the lack of tonic inhibition could place these interneurons in a failsafe mode, ensuring that they can be readily activated (Vardya et al., 2008). Conversely, the low level of tonic inhibition also could leave these neurons with limited ability to control their activity during excessively strong stimulation, contributing to their vulnerability in hyperexcitable pathological conditions.

$GABA_A$R subunits can be introduced selectively in interneurons through Cre-dependent viral transfection in Cre-expressing mice

Although $GABA_A$R subunits have been expressed ectopically *in vivo* in previous studies, either through creation of transgenic mice in which the $\alpha6$ or δ subunit was expressed in broad groups of neurons in the hippocampus and cerebral cortex (Lüscher et al., 1997; Wisden et al., 2002), or through viral transfection of the $\alpha1$ subunit in the dentate gyrus, using the $\alpha4$ $GABA_A$R subunit promoter to drive expression (Raol et al., 2006), the current methods are unique in directing expression of $GABA_A$R subunits to specific subtypes of inhibitory interneurons. These methods for AAV-mediated delivery of Cre-dependent constructs have broad applicability for introducing other $GABA_A$R subunits and using additional mouse

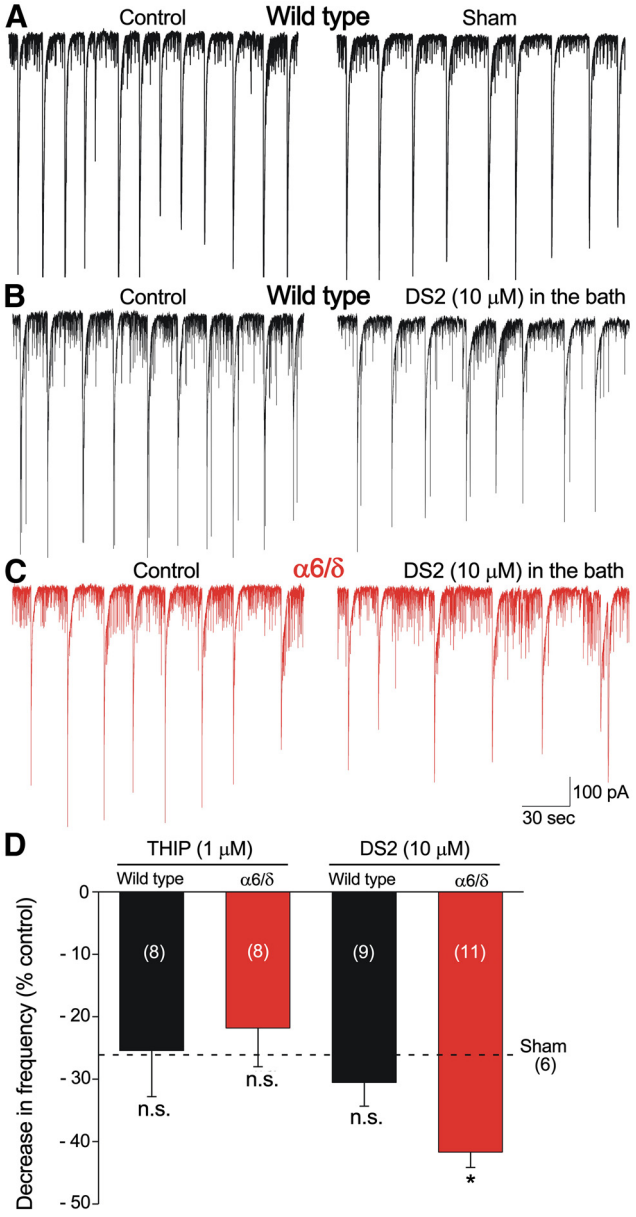

Figure 9. Transfection of hilar SOM neurons with α6/δ renders the 4-AP-activated network sensitive to the allosteric modulator DS2. ***A–C***, Representative traces recorded from granule cells in 4-AP. ***A***, ***B***, Black traces are from wild-type (YFP-transfected and nontransfected tissue). ***C***, Red traces are from α6/δ-transfected tissue. The "Control" conditions on the left are taken from time periods 0–5 min after 4-AP application. Traces corresponding to the indicated pharmacological treatments on the right are taken 5–10 min later. Sham treatments are used to measure the time-dependent decrement in bursting frequency that occurs in slices from both wild-type and α6/δ-transfected animals; these allow estimation of the average rundown and serve as the baseline on which drug effects were discerned (dotted line labeled "Sham" in ***D***). ***D***, Bar graph illustrates mean changes in bursting frequency from control caused by THIP or DS2. Black bars represent nontransfected slices. Red bars represent α6/δ-transfected slices. THIP is ineffective in both networks, and DS2 is ineffective in nontransfected slices but reduces bursting frequency in α6/δ-transfected slices. *$p < 0.05$. n.s., Not significant.

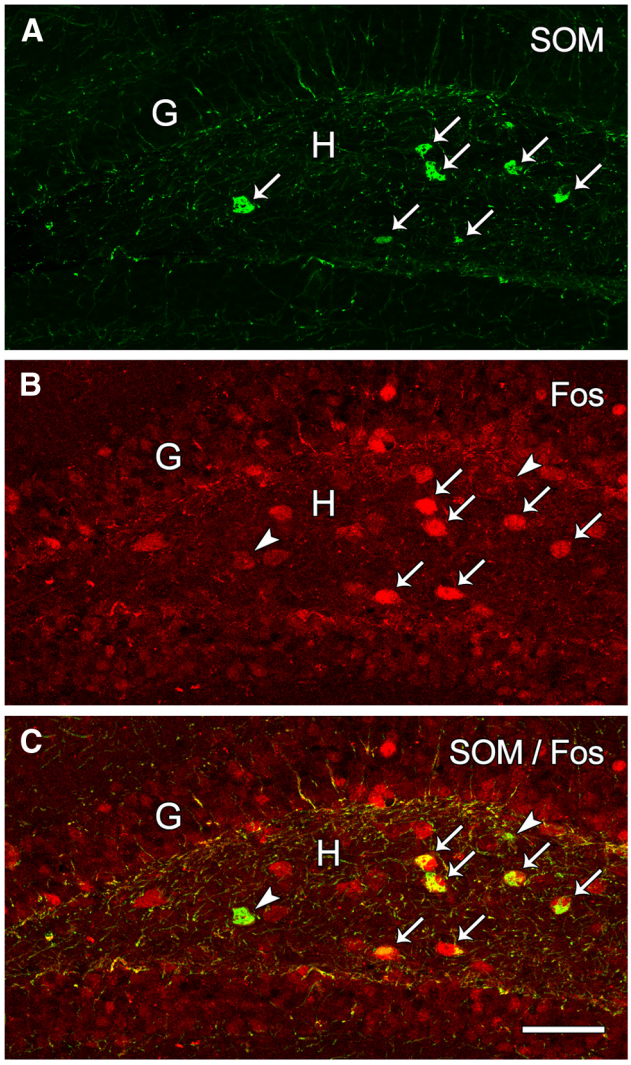

Figure 10. Fos labeling is high in many hilar SOM neurons following PTZ-induced seizure activity in SOM-Cre (nontransfected) animals. ***A***, A number of immunolabeled SOM neurons (arrows) are evident within the dentate hilus (H). ***B***, At 1 h after PTZ injection, a high proportion of the SOM neurons are strongly labeled for Fos (arrows), whereas a few of the SOM neurons exhibit lower or no detectable Fos labeling (arrowheads). Fos labeling is also evident in non-SOM neurons within the hilus (H) and granule cell layer (G). ***C***, Merged images demonstrate that the majority of hilar SOM neurons exhibit strong Fos labeling (arrows) at 1 h after PTZ-induced seizure activity, with a smaller proportion of SOM neurons showing low Fos labeling (arrowheads). Scale bars: (in ***C***) ***A–C***, 50 μm.

lines in which Cre is expressed selectively in specific populations of neurons.

Tonic inhibition in interneurons can be increased by Cre-dependent viral expression of nonsynaptic $GABA_A$R subunits

While immunohistochemistry demonstrated strong expression of the transfected subunits, the formation of functional $GABA_A$Rs was not assured because it would be necessary for the ectopic subunits to assemble into heteromultimeric receptors, traffic to the cell surface, and insert into the plasma membrane at synaptic or nonsynaptic locations (Tretter and Moss, 2008; Macdonald and Kang, 2009). Also, because the formation of functional $GABA_A$Rs requires appropriate subunit partnership, the transfection of a single $GABA_A$R subunit could be insufficient. This was a particular concern with transfection of the δ subunit, as this subunit has been notoriously difficult to incorporate completely and consistently in recombinant $GABA_A$Rs *in vitro* (Meera et al., 2010) and is found almost exclusively associated with α4 or α6 subunits in principal cells (for review, see Olsen and Sieghart, 2009). Nevertheless, *in vivo* transfection of the δ subunit alone led to an approximately sevenfold larger tonic current than that in eYFP control-transfected SOM neurons, indi-

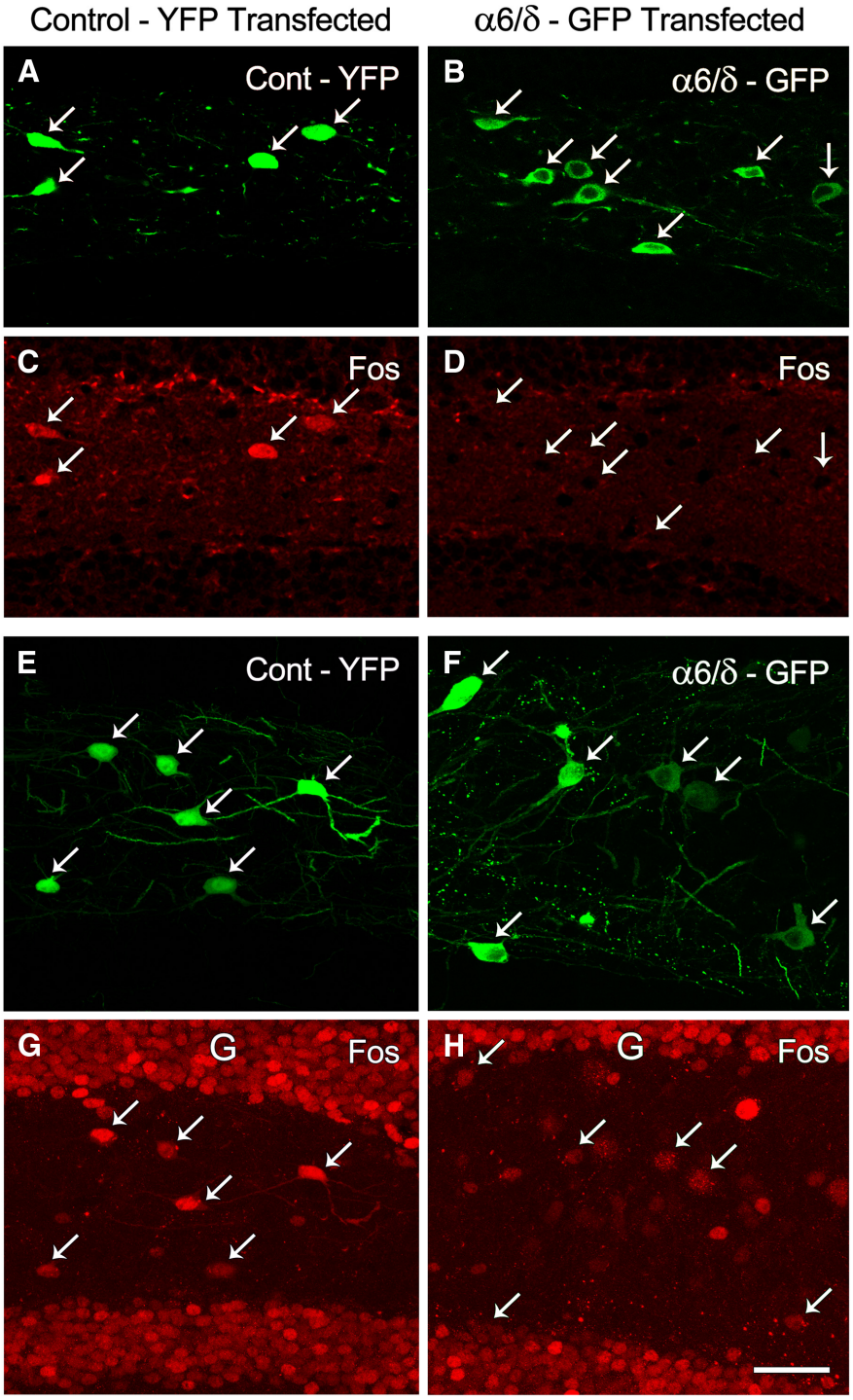

Figure 11. Fos labeling in hilar SOM neurons following PTZ-induced seizure activity is lower in α6/δ-GFP-transfected neurons than in neurons transfected with control YFP. ***A***, ***C***, Control YFP-transfected neurons (***A***, arrows) are each labeled for Fos (***C***, arrows). ***B***, ***D***, In contrast, in α6/δ-GFP-transfected neurons from the same section (***B***, arrows), Fos labeling is virtually absent in the transfected neurons (***D***, arrows). ***E***, ***G***, In another animal in which seizure activity appears to have been more severe, as indicated by Fos labeling of granule cells (G), all control YFP-transfected neurons (***E***, arrows) are labeled for Fos (***G***, arrows). ***F***, ***H***, In α6/δ-GFP-transfected neurons from the same section (***F***, arrows), Fos labeling is generally lower (***H***, arrows) than in control transfected neurons on the contralateral side (compare Fos labeling in ***G***, ***H***). Scale bar: (in ***H***) ***A–H***, 40 μm.

cating that the δ subunit had assembled with endogenous α and β $GABA_A$R subunits.

Transfection for the α6 subunit alone led to substantially larger tonic current than that obtained in δ subunit-transfected neurons. This more robust tonic current could be related to the propensity of the α6 subunit to assemble with several different subunits, as observed in native cerebellar granule cells where α6βδ, α6βγ2, and α1α6βγ2 $GABA_A$Rs have been described (Nusser et al., 1998). Alternatively, it could be related to the much higher affinity α6-containing receptors exhibit for GABA (Meera et al., 2011). In previous studies of a transgenic mouse in which the α6 $GABA_A$R subunit was expressed under control of the Thy1.2 promoter (Thy1α6), the subunit was expressed ectopically in CA1 pyramidal cells and formed functional extrasynaptic receptors that were considered to be mainly α6βγ2 or α6β $GABA_A$Rs (Wisden et al., 2002; Sinkkonen et al., 2004). Similar α6 subunit partnerships are likely in the current study.

Cotransfection of α6 and δ subunits led to the largest tonic current, demonstrating that the high transfection efficiency achieved with AAV-mediated viral transfection allows multiple subunits to be introduced into Cre-expressing neurons. The findings are consistent with preferential assembly of the δ subunit with the α6 subunit, as observed in previous immunoprecipitation experiments (Jechlinger et al., 1998; Pöltl et al., 2003). The δ and α6 subunits coassemble in cerebellar granule cells *in vivo*, and their preferential partnership is emphasized by the nearly complete loss of δ subunit expression in the cerebellar cortex of mice with inactivation of the α6 gene (Jones et al., 1997; Nusser et al., 1999). Thus, it is highly likely that the transfected α6 and δ subunits assembled in the same functional $GABA_A$R, leading to larger tonic currents, possibly greater numbers of functional receptors, and/or increased sensitivity of α6βδ $GABA_A$Rs.

Transfected α6 and δ subunits are localized at nonsynaptic sites in hilar SOM neurons

The preference of the transfected subunits for nonsynaptic rather than synaptic locations is consistent with the normal location of both the α6 and δ subunits. In granule cells of the cerebellar cortex and dentate gyrus, the δ subunit is found nearly exclusively at extrasynaptic and perisynaptic locations (Nusser et al., 1998; Wei et al., 2003). Likewise, in cerebellar granule cells, the α6 subunit is located predominantly at nonsynaptic locations, although localization directly at synapses can occur (Nusser et al., 1996; Santhakumar et al., 2006). A predominantly nonsynaptic localization of the α6 subunit was also observed

when this subunit was expressed ectopically in hippocampal neurons in Thy1α6 transgenic mice (Wisden et al., 2002), and recent *in vitro* studies suggest that the α6 subunit may promote extrasynaptic location of $GABA_A$Rs (Wu et al., 2013).

Phasic inhibition is decreased in SOM neurons cotransfected with α6 and δ subunits

The increase in tonic inhibition in cotransfected neurons was accompanied by a significant decrease in phasic inhibition, as demonstrated by a decrease in sIPSC frequency in the transfected neurons. A similar decrease in IPSC frequency was observed in CA1 pyramidal cells in transgenic Thy1α6 mice (Wisden et al., 2002) and following overexpression of extrasynaptic $\alpha6\beta3\delta$ $GABA_A$Rs in mouse hippocampal neurons in culture (Wu et al., 2013). These previous studies of principal cells have prompted others to hypothesize a homeostatic mechanism by which the neuron's total inhibition is maintained, either by some cell intrinsic regulatory mechanisms (Wisden et al., 2002) or as a result of limited receptor slots on the cell surface (Wu et al., 2013). However, in the present study of interneurons, a plausible explanation is that increased tonic current in SOM interneurons reduced their spontaneous spiking activity and thus their inhibitory synaptic input onto interconnected SOM neurons, contributing to the observed decrease in sIPSC frequency.

Increased tonic inhibition in hilar SOM neurons alters circuit activity in the dentate gyrus *in vitro*

To study the circuit effects of ectopic expression of the α6 and δ subunits in SOM neurons, we selected an *in vitro* experimental paradigm in which the potassium channel blocker 4-AP, in the presence of glutamate receptor blockers, induces $GABA_A$R-mediated bursting in dentate granule cells (Otis and Mody, 1992; Avoli et al., 1996). We hypothesized that an increase in tonic inhibition in the hilar SOM neurons would reduce their activity, leading to a reduction in synchronous firing among these hilar neurons and a decrease in the frequency of $GABA_A$R-mediated bursting in dentate granule cells. Indeed, in hippocampal slices from $\alpha6/\delta$-transfected animals, the frequency of such bursting in dentate granule cells was significantly reduced.

Although the current 4-AP experiments do not mirror normal physiological conditions *in vivo*, the findings suggest a role for tonic inhibition in regulating excessive, synchronous activity among interneurons. Whereas parvalbumin-expressing basket cells are known to promote synchronous activity within many neuronal networks (Cobb et al., 1995; Mann et al., 2005; Bartos et al., 2007), the current and other recent findings suggest that SOM interneurons also could contribute to neuronal synchrony when excessively stimulated (Fanselow et al., 2008; Grosser et al., 2014; Yekhlef et al., 2015).

Increased tonic inhibition in hilar SOM neurons reduces their activation during induced seizure activity *in vivo*

Our in *vivo* findings strongly suggest that increased tonic inhibition in SOM hilar interneurons reduces their activation within an intact circuit during periods of intense stimulation. Such control could be most important during strong stimulation, when SOM neurons can fire synchronously and, despite their normal inhibitory function, contribute to the synchronous firing of granule cells. Similar patterns of activation have been described in cerebellar Purkinje cells that normally fire asynchronously and provide inhibitory control of neurons in the deep cerebellar nuclei but can fire synchronously and, during synchronized periods lacking spikes, induce burst firing in these same neurons (Person and Raman, 2012; Lee et al., 2015).

A role for tonic inhibition in controlling such synchronous activity is supported by recent findings that tonic conductance can control interneuron firing patterns and synchronization in CA3 interneurons bidirectionally, with increased tonic conductance favoring a decrease in synchrony (Pavlov et al., 2014). Thus, the current findings raise the interesting possibility that increasing tonic inhibition in some groups of interneurons could not only limit their firing during strong stimulation but also contribute to the control of excessive synchrony within the network.

References

Avoli M, Barbarosie M, Lücke A, Nagao T, Lopantsev V, Köhling R (1996) Synchronous GABA-mediated potentials and epileptiform discharges in the rat limbic system in vitro. J Neurosci 16:3912–3924. Medline

Bartos M, Vida I, Jonas P (2007) Synaptic mechanisms of synchronized gamma oscillations in inhibitory interneuron networks. Nat Rev Neurosci 8:45–56. CrossRef Medline

Brickley SG, Mody I (2012) Extrasynaptic $GABA_A$ receptors: their function in the CNS and implications for disease. Neuron 73:23–34. CrossRef Medline

Bright DP, Smart TG (2013) Methods for recording and measuring tonic $GABA_A$ receptor-mediated inhibition. Front Neural Circuits 7:193. CrossRef Medline

Buckmaster PS, Dudek FE (1997) Neuron loss, granule cell axon reorganization, and functional changes in the dentate gyrus of epileptic kainate-treated rats. J Comp Neurol 385:385–404. CrossRef Medline

Cobb SR, Buhl EH, Halasy K, Paulsen O, Somogyi P (1995) Synchronization of neuronal activity in hippocampus by individual GABAergic interneurons. Nature 378:75–78. CrossRef Medline

Esclapez M, Chang DK, Houser CR (1996) Subpopulations of GABA neurons in the dentate gyrus express high levels of the α1 subunit of the $GABA_A$ receptor. Hippocampus 6:225–238. CrossRef Medline

Fanselow EE, Richardson KA, Connors BW (2008) Selective, state-dependent activation of somatostatin-expressing inhibitory interneurons in mouse neocortex. J Neurophysiol 100:2640–2652. CrossRef Medline

Farrant M, Nusser Z (2005) Variations on an inhibitory theme: phasic and tonic activation of $GABA_A$ receptors. Nat Rev Neurosci 6:215–229. CrossRef Medline

Ferando I, Mody I (2014) Interneuronal $GABA_A$ receptors inside and outside of synapses. Curr Opin Neurobiol 26:57–63. CrossRef Medline

Fritschy JM, Mohler H (1995) $GABA_A$-receptor heterogeneity in the adult rat brain: differential regional and cellular distribution of seven major subunits. J Comp Neurol 359:154–194. CrossRef Medline

Glykys J, Peng Z, Chandra D, Homanics GE, Houser CR, Mody I (2007) A new naturally occurring $GABA_A$ receptor subunit partnership with high sensitivity to ethanol. Nat Neurosci 10:40–48. CrossRef Medline

Glykys J, Mann EO, Mody I (2008) Which $GABA_A$ receptor subunits are necessary for tonic inhibition in the hippocampus? J Neurosci 28:1421–1426. CrossRef Medline

Grimm D, Lee JS, Wang L, Desai T, Akache B, Storm TA, Kay MA (2008) In vitro and in vivo gene therapy vector evolution via multispecies interbreeding and retargeting of adeno-associated viruses. J Virol 82:5887–5911. CrossRef Medline

Grosser S, Queenan BN, Lalchandani RR, Vicini S (2014) Hilar somatostatin interneurons contribute to synchronized GABA activity in an in vitro epilepsy model. PLoS One 9:e86250. CrossRef Medline

Hadley SH, Amin J (2007) Rat $\alpha6\beta_2\delta$ $GABA_A$ receptors exhibit two distinct and separable agonist affinities. J Physiol 581:1001–1018. CrossRef Medline

Han ZS, Buhl EH, Lörinczi Z, Somogyi P (1993) A high degree of spatial selectivity in the axonal and dendritic domains of physiologically identified local-circuit neurons in the dentate gyrus of the rat hippocampus. Eur J Neurosci 5:395–410. CrossRef Medline

Horton RM, Hunt HD, Ho SN, Pullen JK, Pease LR (1989) Engineering hybrid genes without the use of restriction enzymes: gene splicing by overlap extension. Gene 77:61–68. CrossRef Medline

Houser CR (2014) Do structural changes in GABA neurons give rise to the epileptic state? Adv Exp Med Biol 813:151–160. CrossRef Medline

Jechlinger M, Pelz R, Tretter V, Klausberger T, Sieghart W (1998) Subunit composition and quantitative importance of hetero-oligomeric receptors: $GABA_A$ receptors containing α6 subunits. J Neurosci 18:2449–2457. Medline

Jensen ML, Wafford KA, Brown AR, Belelli D, Lambert JJ, Mirza NR (2013) A study of subunit selectivity, mechanism and site of action of the delta selective compound 2 (DS2) at human recombinant and rodent native $GABA_A$ receptors. Br J Pharmacol 168:1118–1132. CrossRef Medline

Jia F, Pignataro L, Schofield CM, Yue M, Harrison NL, Goldstein PA (2005) An extrasynaptic $GABA_A$ receptor mediates tonic inhibition in thalamic VB neurons. J Neurophysiol 94:4491–4501. CrossRef Medline

Jones A, Korpi ER, McKernan RM, Pelz R, Nusser Z, Mäkelä R, Mellor JR, Pollard S, Bahn S, Stephenson FA, Randall AD, Sieghart W, Somogyi P, Smith AJ, Wisden W (1997) Ligand-gated ion channel subunit partnerships: $GABA_A$ receptor α6 subunit gene inactivation inhibits δ subunit expression. J Neurosci 17:1350–1362. Medline

Lee KH, Mathews PJ, Reeves AM, Choe KY, Jami SA, Serrano RE, Otis TS (2015) Circuit mechanisms underlying motor memory formation in the cerebellum. Neuron 86:529–540. CrossRef Medline

Lee V, Maguire J (2013) Impact of inhibitory constraint of interneurons on neuronal excitability. J Neurophysiol 110:2520–2535. CrossRef Medline

Lee V, Maguire J (2014) The impact of tonic $GABA_A$ receptor-mediated inhibition on neuronal excitability varies across brain region and cell type. Front Neural Circuits 8:3. CrossRef Medline

Li B, Wang L, Sun Z, Zhou Y, Shao D, Zhao J, Song Y, Lv J, Dong X, Liu C, Wang P, Zhang X, Cui R (2014) The anticonvulsant effects of SR 57227 on pentylenetetrazole-induced seizure in mice. PLoS One 9:e93158. CrossRef Medline

Lüscher B, Häuselmann R, Leitgeb S, Rülicke T, Fritschy JM (1997) Neuronal subtype-specific expression directed by the $GABA_A$ receptor delta subunit gene promoter/upstream region in transgenic mice and in cultured cells. Brain Res Mol Brain Res 51:197–211. CrossRef Medline

Macdonald RL, Kang JQ (2009) Molecular pathology of genetic epilepsies associated with $GABA_A$ receptor subunit mutations. Epilepsy Curr 9:18–23. CrossRef Medline

Mann EO, Suckling JM, Hajos N, Greenfield SA, Paulsen O (2005) Perisomatic feedback inhibition underlies cholinergically induced fast network oscillations in the rat hippocampus in vitro. Neuron 45:105–117. CrossRef Medline

Meera P, Olsen RW, Otis TS, Wallner M (2010) Alcohol- and alcohol antagonist-sensitive human $GABA_A$ receptors: tracking δ subunit incorporation into functional receptors. Mol Pharmacol 78:918–924. CrossRef Medline

Meera P, Wallner M, Otis TS (2011) Molecular basis for the high THIP/gaboxadol sensitivity of extrasynaptic $GABA_A$ receptors. J Neurophysiol 106:2057–2064. CrossRef Medline

Milenkovic I, Vasiljevic M, Maurer D, Höger H, Klausberger T, Sieghart W (2013) The parvalbumin-positive interneurons in the mouse dentate gyrus express $GABA_A$ receptor subunits alpha1, beta2, and delta along their extrasynaptic cell membrane. Neuroscience 254:80–96. CrossRef Medline

Nusser Z, Sieghart W, Stephenson FA, Somogyi P (1996) The α6 subunit of the $GABA_A$ receptor is concentrated in both inhibitory and excitatory synapses on cerebellar granule cells. J Neurosci 16:103–114. Medline

Nusser Z, Sieghart W, Somogyi P (1998) Segregation of different $GABA_A$ receptors to synaptic and extrasynaptic membranes of cerebellar granule cells. J Comp Neurol 18:1693–1703. Medline

Nusser Z, Ahmad Z, Tretter V, Fuchs K, Wisden W, Sieghart W, Somogyi P (1999) Alterations in the expression of $GABA_A$ receptor subunits in cerebellar granule cells after the disruption of the α6 subunit gene. Eur J Neurosci 11:1685–1697. CrossRef Medline

Olsen RW, Sieghart W (2009) $GABA_A$ receptors: subtypes provide diversity of function and pharmacology. Neuropharmacology 56:141–148. CrossRef Medline

Otis TS, Mody I (1992) Differential activation of $GABA_A$ and $GABA_B$ receptors by spontaneously released transmitter. J Neurophysiol 67:227–235. Medline

Pavlov I, Savtchenko LP, Song I, Koo J, Pimashkin A, Rusakov DA, Semyanov A (2014) Tonic $GABA_A$ conductance bidirectionally controls interneuron firing pattern and synchronization in the CA3 hippocampal network. Proc Natl Acad Sci U S A 111:504–509. CrossRef Medline

Paxinos G, Franklin KBJ (2001) The mouse brain in stereotaxic coordinates. San Diego: Academic.

Peng Z, Houser CR (2005) Temporal patterns of fos expression in the dentate gyrus after spontaneous seizures in a mouse model of temporal lobe epilepsy. J Neurosci 25:7210–7220. CrossRef Medline

Peng Z, Hauer B, Mihalek RM, Homanics GE, Sieghart W, Olsen RW, Houser CR (2002) $GABA_A$ receptor changes in δ subunit-deficient mice: altered expression of α4 and γ2 subunits in the forebrain. J Comp Neurol 446:179–197. CrossRef Medline

Peng Z, Huang CS, Stell BM, Mody I, Houser CR (2004) Altered expression of the δ subunit of the $GABA_A$ receptor in a mouse model of temporal lobe epilepsy. J Neurosci 24:8629–8639. CrossRef Medline

Peng Z, Zhang N, Wei W, Huang CS, Cetina Y, Otis TS, Houser CR (2013) A reorganized GABAergic circuit in a model of epilepsy: evidence from optogenetic labeling and stimulation of somatostatin interneurons. J Neurosci 33:14392–14405. CrossRef Medline

Peng Z, Tong X, Wallner M, Zhang N, Cetina Y, Otis T, Houser C (2014) Ectopic expression of $GABA_A$ receptor subunits increases tonic inhibition in somatostatin neurons in the hilus of the dentate gyrus. Soc Neurosci Abstr 782:6.

Person AL, Raman IM (2012) Purkinje neuron synchrony elicits time-locked spiking in the cerebellar nuclei. Nature 481:502–505. CrossRef Medline

Pöltl A, Hauer B, Fuchs K, Tretter V, Sieghart W (2003) Subunit composition and quantitative importance of $GABA_A$ receptor subtypes in the cerebellum of mouse and rat. J Neurochem 87:1444–1455. CrossRef Medline

Raol YH, Lund IV, Bandyopadhyay S, Zhang G, Roberts DS, Wolfe JH, Russek SJ, Brooks-Kayal AR (2006) Enhancing $GABA_A$ receptor α1 subunit levels in hippocampal dentate gyrus inhibits epilepsy development in an animal model of temporal lobe epilepsy. J Neurosci 26:11342–11346. CrossRef Medline

Santhakumar V, Hanchar HJ, Wallner M, Olsen RW, Otis TS (2006) Contributions of the $GABA_A$ receptor α6 subunit to phasic and tonic inhibition revealed by a naturally occurring polymorphism in the α6 gene. J Neurosci 26:3357–3364. CrossRef Medline

Savanthrapadian S, Meyer T, Elgueta C, Booker SA, Vida I, Bartos M (2014) Synaptic properties of SOM- and CCK-expressing cells in dentate gyrus interneuron networks. J Neurosci 34:8197–8209. CrossRef Medline

Semyanov A, Walker MC, Kullmann DM (2003) GABA uptake regulates cortical excitability via cell type-specific tonic inhibition. Nat Neurosci 6:484–490. CrossRef Medline

Sinkkonen ST, Vekovischeva OY, Möykkynen T, Ogris W, Sieghart W, Wisden W, Korpi ER (2004) Behavioural correlates of an altered balance between synaptic and extrasynaptic $GABA_A$ergic inhibition in a mouse model. Eur J Neurosci 20:2168–2178. CrossRef Medline

Sun C, Mtchedlishvili Z, Bertram EH, Erisir A, Kapur J (2007) Selective loss of dentate hilar interneurons contributes to reduced synaptic inhibition of granule cells in an electrical stimulation-based animal model of temporal lobe epilepsy. J Comp Neurol 500:876–893. CrossRef Medline

Sun Y, Wu Z, Kong S, Jiang D, Pitre A, Wang Y, Chen G (2013) Regulation of epileptiform activity by two distinct subtypes of extrasynaptic $GABA_A$ receptors. Mol Brain 6:21. CrossRef Medline

Tallent MK (2007) Somatostatin in the dentate gyrus. Prog Brain Res 163:265–284. CrossRef Medline

Tretter V, Moss SJ (2008) $GABA_A$ receptor dynamics and constructing GABAergic synapses. Front Mol Neurosci 1:7. CrossRef Medline

Vardya I, Drasbek KR, Dósa Z, Jensen K (2008) Cell type-specific $GABA_A$ receptor-mediated tonic inhibition in mouse neocortex. J Neurophysiol 100:526–532. CrossRef Medline

Wafford KA, van Niel MB, Ma QP, Horridge E, Herd MB, Peden DR, Belelli D, Lambert JJ (2009) Novel compounds selectively enhance δ subunit containing $GABA_A$ receptors and increase tonic currents in thalamus. Neuropharmacology 56:182–189. CrossRef Medline

Wei W, Zhang N, Peng Z, Houser CR, Mody I (2003) Perisynaptic localization of δ subunit-containing $GABA_A$ receptors and their activation by GABA spillover in the mouse dentate gyrus. J Neurosci 23:10650–10661. Medline

Wei W, Peng Z, Mody I, Houser C (2013) $GABA_A$ receptor mediated tonic currents in five types of neurons of the mouse dentate gyrus. Soc Neurosci Abstr 421:9.

Wisden W, Cope D, Klausberger T, Hauer B, Sinkkonen ST, Tretter V, Lujan R, Jones A, Korpi ER, Mody I, Sieghart W, Somogyi P (2002) Ectopic expression of the $GABA_A$ receptor α6 subunit in hippocampal pyramidal neurons produces extrasynaptic receptors and an increased tonic inhibition. Neuropharmacology 43:530–549. CrossRef Medline

Wu X, Huang L, Wu Z, Zhang C, Jiang D, Bai Y, Wang Y, Chen G (2013) Homeostatic competition between phasic and tonic inhibition. J Biol Chem 288:25053–25065. CrossRef Medline

Wyeth MS, Zhang N, Houser CR (2012) Increased cholecystokinin labeling in the hippocampus of a mouse model of epilepsy maps to spines and glutamatergic terminals. Neuroscience 202:371–383. CrossRef Medline

Yekhlef L, Breschi GL, Lagostena L, Russo G, Taverna S (2015) Selective activation of parvalbumin- or somatostatin-expressing interneurons triggers epileptic seizurelike activity in mouse medial entorhinal cortex. J Neurophysiol 113:1616–1630. CrossRef Medline

Yu J, Proddutur A, Elgammal FS, Ito T, Santhakumar V (2013) Status epilepticus enhances tonic GABA currents and depolarizes GABA reversal potential in dentate fast-spiking basket cells. J Neurophysiol 109:1746–1763. CrossRef Medline

Zhang N, Houser CR (1999) Ultrastructural localization of dynorphin in the dentate gyrus in human temporal lobe epilepsy: a study of reorganized mossy fiber synapses. J Comp Neurol 405:472–490. CrossRef Medline